Available online at www.sciencedirect.com
ScienceDirect
Journal of Magnetic Resonance 189 (2007) 59–77
JMR Journal of Magnetic Resonance
www.elsevier.com/locate/jmr

Simulation of slow-motion CW EPR spectrum using stochastic Liouville equation for an electron spin coupled to two nuclei with arbitrary spins: Matrix elements of the Liouville superoperator

Sushil K. Misra *

Department of Physics, Concordia University,1455 de Maisonneuve Boulevard West, Montreal, Que., Canada H3G 1M8

Received 24 April 2007; revised 29 July 2007
Available online 14 August 2007

Abstract

An algorithm is developed that extends the well known nitroxide slow-motional continuous wave electron paramagnetic resonance (EPR) simulation technique developed originally by Meirovitch et al. [E. Meirovitch, D. Inger, E. Inger, G. Moro, J.H. Freed, J. Chem. Phys. 77 (1982) 3915–3938], and implemented by Schneider and Freed [D.J. Schneider, J.H. Freed, Calculating slow motional magnetic resonance spectra: a user's guide, in: Biological Magnetic Resonance, vol. 6, Plenum Publishing Corporation, 1989]. This paper deals with the more general case of coupling of one electron spin to two nuclear spins. A complete listing of the matrix elements of the Liouville superoperator for this extension has been included. This advance has been successfully tested by reproducing the observed spectral line-shapes of a solution of the novel radical $Mes^*(CH_3)P\text{-}PMes^*$ [$Mes^* = 2,4,6\ (tBu)_3C_2H_2$] in tetrahydrofuran (THF), in which the radical is undergoing slow tumbling, with the coupling of one electron spin to two physically and magnetically inequivalent phosphorus (^{31}P) nuclei.

Keywords: Simulation of EPR spectrum; Slow-motion spectrum; Stochastic Liouville equation; One electron spin coupled to two nuclear spins; Solution of the radical $Mes^*(CH_3)P\text{-}PMes^*$ [$Mes^* = 2,4,6\ (tBu)_3C_2H_2$] in tetrahydrofuran, Directed signature; Threshold directed signature; Bilinear pairings; Provable security

1. Introduction

The detailed theory for the interpretation of EPR spectra of spin labels in the slow motional regime was described by Freed [1], and was widely used in studies in a large variety of domains, such as protein conformations, membrane fluidity and local order, and transition phases in various materials. This advance was further augmented by the powerful computational algorithms, e.g. Lanczos algorithm, specifically adapted to solve these types of problems [2,3], leading to feasible computer time and memory requirements. Now, with the development of extremely fast processors with parallel-processing capability, this aspect is no longer a challenge. Thus, one can now incorporate more sophisticated models of molecular structure and dynamics into line-shape calculation programs. For example, see Liang et al. [4] for models of molecular structure and dynamics for slowly relaxing local structure (SLRS); Polimeno et al. [5] for the SLRS model of solvent cage effects; Liang et al. [6] and Barnes et al. [7] for time resolution analysis to study functional dynamics of proteins *via* augmented stochastic models, and Freed [8] and Borbat et al. [9] for a review of EPR and molecular dynamics. More recently, Barone and Polimeno [10] have provided details of an integrated computational approach incorporating slow-motion simulation towards CW-EPR spectroscopy in dealing with labelled peptides and proteins studied *via* site-directed spin labelling (SDLS). To this end, they have

* Fax: +514 848 2828.
E-mail address: skmisra@alcor.concordia.ca

1090-7807/$ - see front matter © 2007 Elsevier Inc. All rights reserved.
doi:10.1016/j.jmr.2007.08.004

exploited Fourier–Laplace spectral density of generic correlation function in the context of many-body Fokker–Planck models, and simulated EPR spectra as the Fourier–Laplace transform of the correlation function for the x-component of the magnetization starting vector. As illustration, they simulated EPR spectra of a system consisting of one electron spin coupled to two nuclei, as well as to a system containing two coupled nitroxides, incorporating coupling of two electrons and two nuclei including the dipolar interaction between the two electrons.

The ability to simulate and do least-squares fitting of slow-motion spectra is now routine with a nitroxide probe in many biological and other samples in the study of structural ordering and dynamics of the sample [8]. Slow-motion theory has been extensively used to study the properties of NO spin probe interacting with its environment. However, these techniques have not been applied in the past to study spin probes involving coupling of one electron spin to two nuclear spins. The novel approach described in detail here will expand the possible spin probes that may be used in EPR studies. Originally, a suite of codes were written by Moro [11–14], including that by Meirovitch et al. [11] for EPR lineshape calculations based on stochastic Liouville equation, and which were later implemented by Schneider and Freed [15,16], and further exploited by Lee et al. [17] for Fourier transform EPR. The software developed by Schneider and Freed [15] (hereafter SF) is capable of simulating EPR spectra characterized by slow or fast molecular motions, and weak microwave fields, in the limit of high static magnetic fields, which include those required at X-band for the NO radical as demonstrated by the examples listed in Table II in [15]. It is not suitable for simulation of CW EPR spectra at low magnetic fields or very fast motional limits due to the omission of non-secular terms in the hyperfine part of the spin Hamiltonian (Appendix A), which become significant under these conditions, especially for X-band spectra of transition metal ions such as Cu^{2+} and VO^{2+}. For fast motion, EPR spectra can be calculated using a motional narrowing theory requiring a much simpler program [15], whereas low-field spectra are calculated by methods similar to those used in the simpler program. In context with SF algorithm, Earle and Budil [18] have recently presented a detailed description of how slow-motional spectra of NO spin-labelled polymers may be analyzed using the SF EPRLL software [15,16] for CW EPR lineshape calculation.

This paper provides the details of the extension of SF algorithm to the case of coupling of one electron spin to two nuclear spins. This opens up the possibility of using spin probes other than those involving the conventional nitroxide radical. In some cases, they may be even more sensitive and/or less invasive than the nitroxide radical. The model used is briefly described in Section 2. A short review of the SF algorithm is provided in Section 3, with the detailed mathematical formulations of the extension to coupling with two nuclei, based on those given in [11,16] for coupling to one nucleus, are given in Appendices A,B,C. In Section 4 are provided the details of calculation of slow-motion EPR spectrum using the extended SF algorithm [15] to take into account inclusion of a second nuclear spin. Application of the extension to the simulation of the EPR spectra of the di-phosphanyl radical (hereafter radical **1***) contained within the radical $Mes^*(CH_3)P\text{-}PMes^*$ [$Mes^* = 2,4,6\ (tBu)_3C_2H_2$; tBu = *tert-butyl*] (Fig. 1), consisting of spin-1/2 electron spin coupled to two ^{31}P nuclei, is described in Section 5. The concluding remarks are made in Section 6.

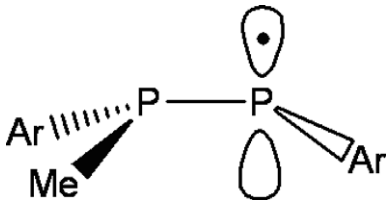

Fig. 1. Configuration of the di-phosphanyl radical. Here Ar denotes the aryl group Mes^* (=2,4,6 $(tBu)_3C_2H_2$).

2. Brief review of the model

The case of rotation of a molecule containing a spin-1/2 electron paramagnetic spin *rigidly connected to two paramagnetic nuclei* with arbitrary spins in a solution is considered. This represents, therefore, the same system as that considered in [11–15] insofar as the non-magnetic part of the molecule is concerned, the only difference being in the electron–nuclear spin part, which now consists of two nuclei instead of one, *both rigidly attached to the electron spin*. Therefore, in the extension to coupling with two nuclei, only one set of stochastic orientational variables are required for the system, the same as that described in [11–15]. Here, one needs only to modify the magnetic part involving the spin Hamiltonian. This requires consideration of two hyperfine interactions of the electron spin with the two nuclei and the two nuclear Zeeman interactions in the enlarged spin space to accommodate the second nuclear spin. As the two nuclei are situated at different spatial locations they are considered statistically ''distinguishable'', or ''inequivalent'', not requiring any symmetrization (or antisymmetrization) of their wavefunctions.

3. Simulation of EPR spectrum due to slow tumbling

Simulation of slow-motion spectra for the case of one electron spin coupled to two nuclei with arbitrary spins is here carried out by extending the expressions given in [11], which treated the case of a radical characterized by an electron spin $S = 1/2$ coupled to a single nucleus with arbitrary spin value (I). In what follows, complete expressions for the extended EPR simulation of a CW EPR spectrum are provided. (The present paper should be read in

conjunction with [11,16] for a complete understanding of the background theory and list of references.) In order to carry out the extension to coupling of one electron ($S = 1/2$) to two nuclei with arbitrary spins (I_1, I_2), one needs to solve the stochastic Liouville equation (SLE) to calculate the time evolution of the relevant density matrix from which the unsaturated high-field, frequency-swept spectrum can be calculated as [11,15]:

$$I(\omega - \omega_0) = \left(\frac{1}{\pi}\right)\langle\langle v|[\tilde{\Gamma} - \mathrm{i}L) + \mathrm{i}(\omega - \omega_0)1]^{-1}|v\rangle\rangle. \qquad (1)$$

In Eq. (1), $\mathrm{i} = \sqrt{-1}$; ω is the sweep frequency, $\omega_0 = g_0\mu_B B/\hbar$, where B is the static magnetic field; $g_0 = (g_{xx}+g_{yy}+g_{yy})/3$ is the average of the three principal values of the g-matrix; μ_B is the Bohr magneton; $\hbar$ is the Planck's constant divided by 2π; L is the Liouville superoperator (LSO) associated with the orientation-dependent spin Hamiltonian; $\tilde{\Gamma}$ is the "symmetrized" diffusion operator used to model the classical reorientational motion; 1 is the identity operator on the right hand side of Eq. (1); $|v\rangle$ is the starting vector that includes the spin operators for the electron and the two nuclei for the allowed EPR transitions and the equilibrium probability distribution function for the orientation of the radical in Liouville space. The special operator $(\tilde{\Gamma} - \mathrm{i}L)$ is commonly referred to as the stochastic Liouville operator (SLO). The details of the reorientational dynamics of the spin label are given in Appendix A, which also includes the required matrix elements of the Liouville spin operator, for the system of one electron spin coupled to two nuclear spins considered here.

4. Procedure to calculate a slow-motion CW EPR spectrum of one electron spin coupled to two nuclei by extended SF algorithm

Brief details of the procedure to calculate slow-motion CW EPR spectrum using the SF algorithm as described in [15] are given here for the sake of completeness. Three subroutines are executed in succession: (i) The parameter-input subroutine LBLL; (ii) The subroutine EPRLL (or EPRCGL), which, among others, calculates the matrix elements of the SLO for spectral calculation and the elements of the starting vector, wherein the matrix of the SLO is tridiagonalized by either complex-symmetric Lanczos or conjugate-gradient algorithm; and (iii) the subroutine TDLL, which processes the Lanczo's tridiagonal matrix generated by EPRLL/EPRCGL to calculate the CW EPR spectrum by evaluating the continued-fraction representation of the spectral function whose elements are defined by the matrix elements of the Lanczos tridiagonal matrix. These subroutines call, in turn, other subroutines to perform the intended tasks. An important subroutine is MATRLL which calculates the required elements of the spin-Hamiltonian matrix. The subroutine STVECT calculates the elements of the starting vector required for Lanczos algorithm, consisting of nine nested loops over $L, K, M, p^S, q^S, p^{I_1}, q^{I_1}, p^{I_2}, q^{I_2}$ indices, where the spin indices $p^S, q^S, p^{I_1}, q^{I_1}, p^{I_2}, q^{I_2}$ depend on electronic and nuclear magnetic quantum numbers as defined in Appendix A. The subroutines responsible for Lanczos and complex-gradient algorithms are SLNZS and CSCG, which tridiagonalize arbitrary square matrices and solve the required linear systems of algebraic equations, respectively. All the required subroutines were appropriately modified here from those of the SF source code to include the second nuclear spin. The three executable files for simulation of EPR spectrum can be compiled on a reasonably powerful personal computer equipped with a Fortran compiler. For simulation of EPR spectrum by the use of these executable files, available from the author, one does not need a compiler; only a personal computer is required, and one needs just to enter the required input parameters.

5. Illustrative example: Simulation of spectra for the phosphonic radical 1*

A complete experimental EPR study for the case of one electron spin coupled to two nuclear spins in the 100–300 K range was made by Cataldo et al. [19], which should be referred to for experimental details. The phosphonic radical was found to be stable in solution in THF due to the presence of the sterically demanding aryl group, 2,4,6-tri (*tert-butyl*) benzene, called Mes*, which protects the dicoordinated phosphorus atoms efficiently. They found for this sample that for temperatures less than 160 K and greater than 180 K, there exist effects, over and above those governed by the framework of "slow motion", which dominate the EPR spectrum. It is only over the temperature interval 160–180 K for which the slow motion is the principal mechanism dictating the EPR spectrum. In this radical, the electron is delocalized in a phosphorus–phosphorus π radical, coupled to two magnetically inequivalent ^{31}P nuclei located at physically distinct sites (Fig. 1), each with spin 1/2. It is this system of one electron spin coupled to two spin-1/2 nuclei, which produces the EPR spectrum. The elements of the $\tilde{g}$ and the two $\tilde{A}$ matrices, which are all symmetric, for the radical **1*** as determined experimentally for a *single crystal* of diphosphane Mes*(CH$_3$)P-PMes* grown in the presence of the radical **1*** placed at an arbitrary orientation in the laboratory frame (L: x, y, z; the z-axis being parallel to the external magnetic field) are listed in Table 1 here as taken from [19].

From the above values of the matrix elements it is clear that, for the particular chosen orientation of the crystal with respect to the external magnetic field to determine the $\tilde{g}$ and the two $\tilde{A}$ matrices, the laboratory frame is not coincident with the principal-axes frame of any one of the three matrices. This has here been taken into account by using the complete set of irreducible spherical tensor operators (ISTO) components, including the off-diagonal elements of the $\tilde{g}$ and the two $\tilde{A}$ matrices as listed in Appendix B. These values were used in the subroutines LBLL/MATRLL for the calculation of the relevant

Table 1
Parameters used for simulations of slow-motion CW EPR spectra (listed in the same way as in [11])

g-Tensor [g_{xx}, g_{yy}, g_{zz}, g_{zx}, g_{zy}, g_{xy}]:	2.0157	2.0024	2.0061	−0.0060	0.0012	0.0000	
Twice the first nuclear spin [in21]:	1						
A_1-tensor [$axx1$, $ayy1$, $azz1$, $azx1$, $azy1$, $axy1$] (gauss):	121.600	161.300	134.800	0.370	−30.300	2.700	
Twice the second nuclear spin [in22]:	1						
A_2-tensor [$axx2$, $ayy2$, $azz2$, $azx2$, $azy2$, $axy2$] (gauss):	10.000	234.600	12.600	−7.000	−31.900	26.500	
Static field [B] (Gauss):	3364.00						
Diffusion parameter [ipdf] =	0						
Heisenberg spin exchange frequency [oss] =	0.000						
Number of terms in the potential [ipt] =	0						
Angle between B and local director [psi] (degrees):	0.00						
Diffusion tilt index [itd] =	0						
Magnetic tilt index [itm] =	0						
Truncation values [lemx, lomx, kmx,mmx,ipnmx1, ipnmx2, ipemn]:	12	7	2	2	1	1	1
L+K+M truncation rule flag [lkmtrc]:	0						
Number of Lanczos/CG steps [nstep]:	200						
Calculation type (0 = L, 1 = CG, 2 = FS) [itype]:	0						

spin-Hamiltonian matrix elements. They lead to a good simulation of the features of the EPR spectra observed between 160 and 180 K for radical $\mathbf{1}^*$ in solution, so that the shapes of the simulated slow-motion spectra can be made to correspond well to those observed experimentally, as shown in Fig. 2, by appropriate choices of the isotropic diffusion rate $d(=d_{xx} = d_{yy} = d_{zz})$ varying between 1.0 and 6.0×10^8 s^{-1}. It is noted, in particular, that the variation of d value not only affects the line-width of the signals but also the number of the EPR lines constituting the spectrum, in accordance with the experimental spectra. Fig. 2 shows the simulations for particular chosen values of d. These appear to reproduce approximately the recorded experimental data at selected temperatures. It is clear that upon finer variations of the parameter values for d_{xx}, d_{yy}, d_{zz} the simulated spectra can be made to correspond well to those observed experimentally. To this end, one can use the least-squares fitting technique.

At 160 K, the experimental spectrum of $\mathbf{1}^*$ is composed of seven lines which are approximately reproduced in the simulated spectrum shown in Fig. 2 (isotropic diffusion rate $d = 1.0 \times 10^8$ s^{-1}). At and above 160 K, the sample is probably homogeneous and its reduced viscosity allows the irregularly shaped radical to tumble freely in an isotropic manner. At 165 K, the spectrum is composed of a triplet of doublets. A good simulation of this pattern can be drawn by assuming an isotropic reorientation of the radical with $d = 1.5 \times 10^8$ s^{-1}, not shown here. Increasing the temperature, or equivalently the value of d, causes the external doublets to coalesce progressively, as seen in the simulated spectra in Fig. 2 for $d = 1.75$ and 3.0×10^8 s^{-1}, which correspond to the experimental spectra observed at 175 and 180 K, respectively. By increasing d to 1.0×10^9 and 5.0×10^9 s^{-1}, it is seen that the simulated spectrum consists of only four lines as shown in Fig. 3. The parameters used for these simulations are given in Table 1. These are the same for all simulations shown in Figs. 2 and 3, with only the isotropic parameter d being different. As for adjusting the values of the truncation parameters listed here in Table 1, the initial values of these were chosen to be similar to those listed in Table 2 and Appendix of [15], which were then varied so as to provide the best resemblance to the experimental spectra by *trial-and-error*.

In general, as seen from Fig. 3, increasing the diffusion rate to faster than 6.0×10^8 s^{-1} does not change the number and positions of the lines; it causes only a decrease in their line-widths, making the lines sharper. In the present example, an additional increase in the value of d causes only a narrowing of the line-width of the four peaks in the simulated spectra, similar to that found for the NO radical [15] with the slow-motion mechanism dictating the spectrum. However, with the diphosphanyl radical 1^* spin probe, several drastic physical modifications occur in the radical that affect the experimental spectrum above 185 K, masking seriously the slow-motion features of the EPR spectrum [19].

When comparing the present simulations with those of the NO spectrum with its typical values of the $\tilde{g}$ and the two $\tilde{A}$ matrices [11] for the same values of d, not shown here, it was found that the sensitivity to the motion for the phosphorus containing radical $\mathbf{1}^*$ is considerably larger than that for the nitroxide probe in this motional range. Thus, radical $\mathbf{1}^*$ appears to be more sensitive than the nitroxide radical.

Finally, it is noted that the algorithm presented here reproduces eminently the results for simulation of EPR spectrum for one electron spin coupled to one nuclear spin, e.g. that for a nitroxide radical as given in [11], in the limit when the elements of the $\tilde{A}$ matrix characterizing the second nucleus are made to approach zero.

6. Concluding remarks

The salient features of the simulation technique for the extension proposed in this paper are as follows.

(i) The extension of the SF algorithm to coupling of one electron spin to two nuclei presented here provides the framework for an important extension of the

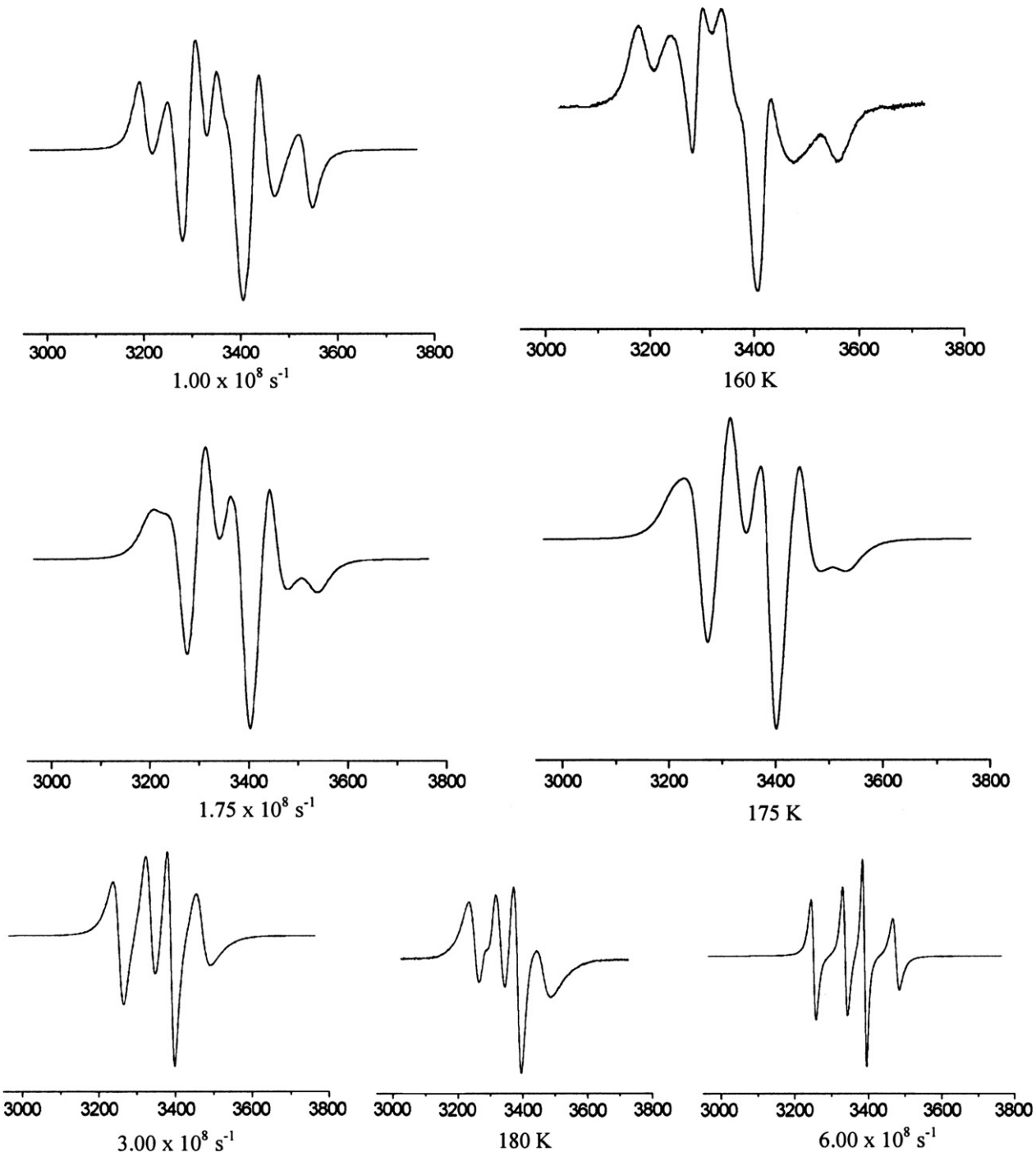

Fig. 2. Simulation of slow-motion EPR spectrum (arbitrary units) as a function of the (isotropic) diffusion parameter d, which depends on temperature, for the radical $Mes^*(CH_3)P\text{-}PMes^*$ [$Mes^* = 2,4,6\ (tBu)_3C_2H_2$] for $d = 1.0$, 1.75, 3.0, and $6.0 \times 10^8\ s^{-1}$. The experimental first-derivative EPR spectrum closest to it in its features is shown to the right of each simulated spectrum. For each simulated spectrum the value of d is given below the figure, while the temperature of the experimental spectrum is indicated below it. The magnetic field shown in the abscissa is in Gauss over the range 3000–3800 G.

algorithm. This involves inclusion of one more electron to treat the case of two electrons coupled to each other, and each electron coupled to a single nucleus. One can then apply that simulation algorithm to bilabeled nitroxides, where the separation of the two electrons has a significant effect on the spectral shape due to the dipolar interaction. This can be exploited to measure distances by fitting to experimental data, e.g. that obtained by pulsed ELDOR. The advantage with the ELDOR technique is that here one makes

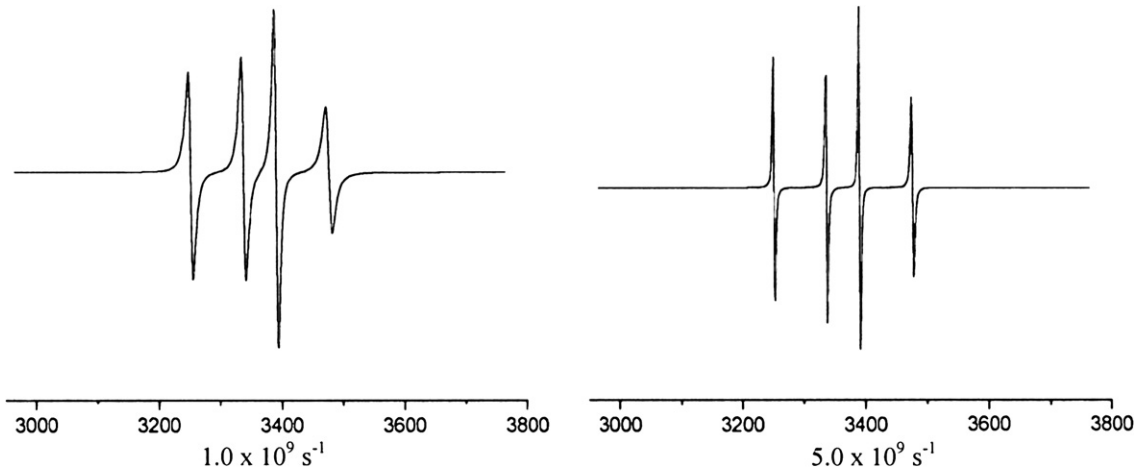

Fig. 3. Simulation of slow-motion EPR spectrum (arbitrary units) as a function of the (isotropic) diffusion parameter d, which varies with temperature, for the radical Mes*(CH_3)P-PMes* [Mes* = 2,4,6 $(tBu)_3C_2H_2$] for $d = 1.0$ and 5.0×10^9 s^{-1}. It shows that for these values as d increases the number of lines remain the same, but the linewidth decreases making the lines sharper. The experimental spectra for these values of d are not available in the slow-motional region due to the other dominant mechanisms operative in the sample, which prevail over the slow motion. The magnetic field shown in the abscissa is in Gauss over the range 3000–3800 G.

measurements in biological samples at *in-vivo* temperatures, unlike the case for double quantum coherence (DQC). Such effort is currently under way.

(ii) The application of the extended algorithm proposed in this paper to coupling of one electron with two nuclei showed that the EPR spectrum of the diphosphanyl radical **1*** is much more sensitive to its tumbling rate than that for the nitroxide radical characterized by coupling of one electron to one nucleus due to the large anisotropy of the ^{31}P couplings [5]. Thus, this, or similar radicals, may have a potential to be used as spin labels, of course, subject to further testing that, indeed, the other required qualities of a spin label are present.

(iii) The algorithm presented here treats the general case of non-coincident principal axes of the $\tilde{g}$ and the two $\tilde{A}$ matrices, taking into account their non-zero off-diagonal elements. To this end, the irreducible spherical tensor operators (ISTO) are listed here as a generalization to [15]. This enables one to transform them directly to the diffusion frame, rather than transforming the matrix elements from the principal-axes frames of the hyperfine matrices to that of the g-matrix, and then transforming to the diffusion frame. Thus, the procedure presented here obviates the need to diagonalize the various matrices.

(iv) Complete sets of the matrix elements of the Liouville and diffusion superoperators have been included in Appendices A,B,C in both the K- and M-symmetrized representations in a consistent manner. There may have been some duplication of the expressions given here with those in [15,16] for the diffusion part, but it is felt that the complete listing given here will prove to be more useful for further exploitation of the technique to extend the present calculation to two coupled NO radicals involving coupling of two electron spins to two nuclear spins. As well, every effort has here been made to correct for the numerous typos in [7].

(v) The algorithm developed here is also applicable to slow-motional NMR spectroscopy. This requires appropriate generalization to take into account the properties of inorganic radicals, e.g. the vanadyl and cupric ions often used in biophysical studies. [See [15], and references therein.]

The author can be contacted to obtain the executable files compiled here for simulation of CW EPR spectra for one electron spin coupled to two nuclear spins.

Acknowledgments

The author is grateful to Professor Jack Freed and Dr. D. Schneider of Cornell University, and to Professor D. Budil of Northeastern University for many significant discussions on the subject. He expresses his gratitude to Professor Michel Geoffroy for drawing his attention to make this extension to interpret the EPR spectrum of the radical **1***, and for financing his sojourn at the University of Geneva in October 2003 for this project. Critical reading of the manuscript and constructive comments to improve the manuscript by Dr. R.H. Crepeau (Ithaca, N.Y.) are greatly appreciated. Partial financial support from the Natural Sciences and Engineering Research Council (NSERC) of Canada is acknowledged.

Appendix A. General expression for CW EPR simulations

This appendix describes the various expressions required in the calculation of a slow motion CW EPR spectrum for the case of one electron spin ($S = 1/2$) coupled to two

nuclear spins with arbitrary spins. The absorption EPR spectrum is expressed as [11]:

$$I(\omega) = \frac{1}{\pi}\mathrm{Re}\{\langle v|[\mathrm{i}(\omega 1 - L) + \Gamma]^{-1}|v\rangle\}, \tag{A1}$$

where Γ is the symmetrized diffusion operator and L is the Liouville operator associated with the Hamiltonian of the magnetic interaction, 1 is the identity operator, and $|v\rangle$ is the unit vector of the allowed EPR transitions in the Liouville space discussed in this appendix.

There are two contributions to this spectral simulation, which arise from: (i) the reorientation dynamics of the spin label; and (ii) the interactions of the spin part of the label. In the theoretical treatment that follows, the tilt of the molecule, ψ, which is the angle between the axis of symmetry of the molecule and the magnetic field, is explicitly taken into account, and the general case is considered, where *the principal axes of the diffusion*, $\boldsymbol{g}$, *and the two* $\boldsymbol{A}$ *tensors are assumed to be non-coincident*.

A.1. Reorientational dynamics

The reorientational dynamics of the (rigid) spin label is modelled by a symmetrized rotational diffusion superoperator with a restoring potential of the form [15]:

$$U(\Omega) = -k_B T\left\{\sum_{L=2,4}\lambda_0^L D_{00}^L(\Omega) + \lambda_2^L\left[D_{02}^L(\Omega) + D_{0-2}^L(\Omega)\right]\right\},$$

where $\Omega = (\alpha, \beta, \gamma)$ represents the set of Euler angles describing the orientation of the radical relative to the laboratory-fixed frame (L). The functions $D_{MK}^L(\Omega)$ are the generalized spherical harmonics or Wigner rotational matrix elements, most convenient to describe the rotational diffusion process, which is the most important source of relaxation. In particular, for $M = 0$,

$$D_{0K}^L(\Omega) = \left(\frac{4\pi}{2L+1}\right)^{1/2} Y_{LK}(\beta, \gamma),$$

where $Y_{LK}(\beta, \gamma)$ are the well known spherical harmonics. Such a restoring potential is appropriate for modelling the rotational dynamics of spin probes in uniaxial liquid-crystal media. In addition to diffusion, one may model jump processes between an arbitrary number of equivalent sites, and include Heisenberg spin exchange interaction between neighboring electrons coupled to neighbouring nuclei. The overall "diffusion" operator is the simple superposition of these terms. One can choose between the three canonical models of Brownian, jump, and free diffusion to describe the dynamics of radicals in isotropic media. Explicit expressions and references for these are given below in this appendix. The two most important parameters are the parallel (d_{zz}) and perpendicular (d_{xy}) components of the rotational diffusion tensor. The parallel component is related to the correlation time for the motion of the spin probe about the symmetry axis of the diffusion tensor, whereas the perpendicular component is related to the motion perpendicular to the symmetry axis. For isotropic situation the two components become equal to each other ($d_{zz} = d_{xy} = d$). This simulation is only applicable when the sample is in a liquid state.

The Wigner rotation functions are required, among other things, to transform the second-rank tensor describing the spin Hamiltonian in three successive transformations schematically represented as $m \to R \to d \to L$. Here, L is the laboratory-fixed reference frame wherein the z-axis is along the static magnetic field; d is the director frame whose z-axis is taken to be along the symmetry axis of the restoring potential or along the laboratory frame in the absence of restoring potential; R is the principal-axis frame of the rotational diffusion tensor; and m is defined collectively by the reference frames in which the elements of the $\boldsymbol{g}$ and the two $\boldsymbol{A}$ matrices are determined. It is noted that here the general case is considered, where the principal-axes systems of the $\boldsymbol{g}$ and the two $\boldsymbol{A}$ magnetic tensors are non-coincident, and transformations are made directly from the respective frames, in which the various matrices are experimentally determined, to the R frame. As for the orientations, d, L, and m are space fixed, whereas R is rigidly fixed with respect to the molecular framework and is, therefore, referred to as molecular- or body-fixed frame.

A.2. Matrix elements of the Liouville superoperator

This is an extension of the formalism given by Meirovitch et al. [11] for the extension to an electron spin ($S = 1/2$) coupling to two nuclei with arbitrary spins. (The typographical errors in [7] have been corrected here.)

The spin Hamiltonian is expressed in angular frequency units as:

$$H = \frac{\mu_B}{\hbar} B \cdot \tilde{g} \cdot S + \sum_{i=1,2}(\gamma_e I^i \cdot \tilde{A}^i \cdot S - \gamma_n B \cdot I^i), \tag{A2}$$

where the three terms on the right hand side represent the electronic Zeeman, hyperfine, and (isotropic) nuclear Zeeman interactions, respectively; and the superscripts refer to the two nuclear spins; $\gamma_e (= \frac{\mu_B}{\hbar} g_e)$ and $\gamma_n (= \frac{g_N \mu_N}{\hbar})$ are, respectively, the electronic and nuclear gyromagnetic ratios, with g_N and μ_N being the nuclear g-factor and nuclear magneton, respectively. The operators $\boldsymbol{L}$ and $\boldsymbol{\Gamma}$ appearing in Eq. (A1) are defined in the Liouville space of the product of the normalized Wigner rotation matrices and *spin transitions*:

$$|m^{s'} m^{I_{1'}} m^{I_{2'}}; m^{s''} m^{I_{1''}} m^{I_{2''}}; LMK\rangle$$
$$\equiv |m^{s'} m^{I_{1'}} m^{I_{2'}}; m^{s''} m^{I_{1''}} m^{I_{2''}}\rangle \sqrt{\frac{2L+1}{8\pi^2}} D_{MK}^L(\Omega), \tag{A3}$$

where m^s, m^{I_1}, m^{I_2} are the eigenstates of the spin operators $\boldsymbol{S}_z$, $\boldsymbol{I}_{z1}$, $\boldsymbol{I}_{z2}$:

$$\begin{aligned} S_z|m) &= m|m); \\ I_{z_1}|m^{I_1}) &= m^{I_1}|m^{I_1}); \\ I_{z_2}|m^{I_2}) &= m^{I_2}|m^{I_2}). \end{aligned} \tag{A4}$$

Here, $|\sim)$ denotes kets in Hilbert spin space, whereas $|\sim\rangle$ denotes kets in Liouville spin space.

The correspondence between the matrix elements in the Hilbert space and those in the Liouville space is as follows:

$$(m^{s'}|S|m^{s''}) \rightarrow \langle S|m^{s'}, m^{s''}\rangle, \tag{A5}$$

which shows that $|m^{s'}m^{s''}\rangle$, with the two indices representing the electronic transitions in EPR, is treated as a ket in Liouville space; the nuclear spin transitions are treated in the same way.

A.2.1. Reference frames

The various reference frames used here are as follows.

Laboratory frame (L). It is arbitrary, denoted as (x, y, z), and defined specifically for a particular problem. The magnetic field, B, is assumed to be parallel to the z-axis.

Director frame (d). Denoted as (x'', y'', z''), wherein the z''-axis is parallel to d, the axis of symmetry for a uniaxial liquid crystal. It may be tilted away from the magnetic field by the angle ψ, referred to as the "director tilt".

Diffusion frame (D). Denoted as (x', y', z'), which is the principal-axes frame of the diffusion tensor, R.

Magnetic frames (m). These frames are arbitrary; in the calculations presented here the components of the $\boldsymbol{g}$ and two $\boldsymbol{A}$ matrices are expressed in the laboratory frame as measured for a single crystal of the radical at an arbitrary orientation.

The argument Ω of the Wigner rotation matrices, $D^L_{MK}(\Omega)$, is the set of Euler angles that define the transformation from the d frame to the D frame:

$$\Omega \equiv \Omega_{d\rightarrow \mathrm{D}}. \tag{A6}$$

Then, the α angle in the $\Omega \equiv (\alpha, \beta, \gamma)$ represents the rotation about z''. This transformation renders the non-zero components of the starting vector $|\mathrm{v}\rangle$ to a minimum.

A.2.2. Matrix elements of L

The spin Hamiltonian for the system is expressed in the spherical tensor notation as [7]

$$H(\Omega) = \sum_{\mu,m,\ell} F^{(\ell,m)*}_{\mu,\eta} A^{(\ell,m)}_{\mu,\eta} = \sum_{\mu,m,\ell} (-1)^m F^{(\ell,-m)}_{\mu,\eta} A^{(\ell,m)}_{\mu,\eta}, \tag{A7}$$

where the $F^{(\ell,m)}_{\mu,\eta}$ are proportional to the standard ISTO (irreducible spherical tensor operators) components of the magnetic tensor of the type μ (=$\boldsymbol{g}$, $\boldsymbol{A}_1$, $\boldsymbol{A}_2$, $\boldsymbol{g}_{N1}$, $\boldsymbol{g}_{N2}$) in the reference frame η. The quantities $A^{(\ell,m)}_{\mu,\eta}$ are the ISTO components of the tensors, which arise from the coupling of spin and/or magnetic field operators.

In order to use the non-diagonal matrix elements of the $\boldsymbol{g}$ and $\boldsymbol{A}$ matrices in the laboratory frame (L) in which they are measured in the present case, which is not, in general, the principal-axes frame of these tensors, one needs a complete listing of all the five coefficients $g^{(2,m)}, F^{(2,m)}_{g,L}$, and $F^{(2,m)}_{A,L}(m = \pm 2, \pm 1, 0)$ (A single crystal of the radical was used to measure its $\boldsymbol{g}$ and $\boldsymbol{A}$ tensors at an arbitrary orientation in the spectrometer, which was not coincident with the principal axes of any tensor). In particular, it is noted that the principal axes of the $\boldsymbol{A}$ matrices for the two nuclei are not coincident with each other or with those of the $\boldsymbol{g}$ matrix in the present case. It is, therefore, not necessary to make an extra effort to diagonalize the various matrices, and then transform the (diagonalized) $\boldsymbol{A}$ matrices to the principal-axes frame of the $\boldsymbol{g}$ matrix as was done in [11,15]. Transformations of the matrix elements of these matrices were rather made here directly from the laboratory frame to the director frame (space fixed), and then to the diffusion frame (body fixed). For the general case considered here, all five irreducible spherical tensor operators of second order are required. These are described in Appendix B.

One now uses the transformation property of the spherical components of a tensor in going from frame 2 to 1:

$$F^{(l,m)*}_{\mu,1} = \sum_{m'} D^l_{m,m'}(\Omega_{1\rightarrow 2}) F^{(l,m')*}_{\mu,2}. \tag{A8}$$

The dependence of H on the orientation of the molecule can now be written explicitly as:

$$H = \sum_{\mu,l,m,m',m''} d^l_{m,m'}(\psi) D^l_{m',m''}(\Omega) F^{(l,m'')*}_{\mu,D} A^{(l,m)}_{\mu}, \tag{A9}$$

where ψ is the angle between d and B, and $d^l_{m,m'}(\psi) = D^l_{m,m'}(0, \psi, 0)$.

For simplicity in equations for matrix elements, the indices for the EPR transitions in the Liouville space will be redefined as follows, with $i = s$, I_1, or I_2:

$$\begin{aligned}
&p^i = m^{i'} - m^{i''}: \\
&\quad p^s = -1, 0, 1; \\
&\quad p^{I_1} = -2I_1, -2I_1 + 1, \ldots, 2I_1; \\
&\quad p^{I_2} = -2I_2, -2I_2 + 1, \ldots, 2I_2. \\
&\quad q^i = m^{i'} + m^{i''}: \\
&q^i = -Q^i, -Q^i + 2, \ldots, Q^i; \\
&\quad Q^s = 1 - |p^s|; \\
&\quad Q^{I_1} = 2I_1 - |p^{I_1}|; \\
&\quad Q^{I_2} = 2I_2 - |p^{I_2}|.
\end{aligned} \tag{A10}$$

It is noted that in the CW EPR situation, where the non-secular contributions are usually negligible in the high-field limit, except for very fast motions, the stochastic Liouville matrix is block diagonal in terms of the p^s indices. One can then diagonalize each p^s block separately to obtain the eigenvalues. This is because the basis vectors with different p^s indices are coupled only through the S_+ or S_- operators, appearing only in the non-secular terms in the hyperfine part of the spin Hamiltonian, which are neglected here. Further, for CW EPR $S = 1/2$, thus the $p^s = 0$ basis vectors span the "*diagonal subspace*", containing the diagonal and pseudo-diagonal density matrix elements for which the nuclear indices are both $p^i = 0$ and $p^i \neq 0$ ($i = I_1$ and I_2); and the $p^s = \pm 1$ basis vectors span the two conjugate "*off-diagonal subspaces*".

A.3. Matrix elements of the Hamiltonian superoperator ($H^{\times}$)

According to Eq. (A9) above, the matrix elements of $H^{\times}$ depend on those of the superoperators $(A_{\mu}^{(l,m)})^{\times}$, whose calculation is described in Appendix C. The matrix elements of L ($=H^{\times}$) can now be written as follows:

$$\begin{aligned}&\langle p_1^s q_1^s; p_1^{I_1} q_1^{I_1}; p_1^{I_2} q_1^{I_2}; L_1 M_1 K_1 | H^{\times} | p_2^s q_2^s; p_2^{I_1} q_2^{I_1}; p_2^{I_2} q_2^{I_2}; L_2 M_2 K_2 \rangle \\ &\quad = N_L(L_1, L_2)(-1)^{M_1+K_1} \sum_{\mu,l} \langle p_1^s q_1^s; p_1^{I_1} q_1^{I_1}; p_1^{I_2} q_1^{I_2} | [A_{\mu}^{(l,\Delta p)}]^{\times} \\ &\quad |p_2^s q_2^s; p_2^{I_1} q_2^{I_1}; p_2^{I_2} q_2^{I_2}\rangle \times d^l_{\Delta p, M_1 - M_2}(\psi) F^{(l,K_1-K_2)}_{\mu,D} * \\ &\quad \begin{pmatrix} L_1 & l & L_2 \\ M_1 & M_2 - M_1 & -M_2 \end{pmatrix} \begin{pmatrix} L_1 & l & L_2 \\ K_1 & K_2 - K_1 & -K_2 \end{pmatrix},\end{aligned} \tag{A11}$$

where

$$\begin{aligned}&N_L(L_1, L_2) = (2L_1+1)^{1/2}(2L_2+1)^{1/2} \quad \text{and} \\ &\Delta p = p_1^s + p_1^{I_1} + p_1^{I_2} - p_2^s - p_2^{I_1} - p_2^{I_2}.\end{aligned} \tag{A11a}$$

The symmetry characterizing Eq. (A.11), as deduced from Eq. (C9) of Appendix C, is as follows:

$$\begin{aligned}&\langle -p_1^s, q_1^s; -p_1^{I_1}, q_1^{I_1}; -p_1^{I_2} q_1^{I_2}; L_1, -M_1, -K_1 | L | \\ &\quad - p_2^s, q_2^s; -p_2^{I_1}, q_2^{I_1}; -p_2^{I_2}, q_2^{I_2}; L_2, -M_2, -K_2 \rangle \\ &\quad = (-1)^{1+M_1+M_2+K_1+K_2} \langle p_1^s q_1^s; p_1^{I_1} q_1^{I_1}; p_1^{I_2} q_1^{I_2}; L_1 K_1 M_1 | L | p_2^s q_2^s; \\ &\qquad p_2^{I_1} q_2^{I_1}; p_2^{I_2} q_2^{I_2}; L_2 K_2 M_2 \rangle.\end{aligned} \tag{A12}$$

Substituting $d^l_{\Delta p, M_1 - M_2}(\psi) = \delta_{\Delta p, M_1 - M_2}$ for $\psi = 0$ (absence of director tilt) in Eq. (A.11), which dictates for $\psi = 0$ that $p_1^s + p_1^{I_1} + p_1^{I_2} - M_1 = p_2^s + p_2^{I_1} + p_2^{I_2} - M_2$. Then it is seen from Eq. (A.11) that in this case L is factored into distinct blocks of non-zero matrix elements characterized by linear combination of indices such that:

$$p^s + p^{I_1} + p^{I_2} - M = \text{constant}. \tag{A13}$$

A.4. Matrix elements of $\boldsymbol{\Gamma}$

The complete expression for the stochastic diffusion superoperator including all sources of relaxation is:

$$\boldsymbol{\Gamma} = \boldsymbol{\Gamma}_{\mathbf{iso}} + \boldsymbol{\Gamma}_{\mathbf{U}} + \boldsymbol{\Gamma}_{\mathbf{dj}} + \boldsymbol{\Gamma}_{\mathbf{ex}} + \boldsymbol{\Gamma}_{\mathbf{We}} + \boldsymbol{\Gamma}_{\mathbf{Wn}}. \tag{A14}$$

The various sources of relaxation included in this operator are described below. The spin indices $p_1^s, q_1^s, p_1^{I_1}, q_1^{I_1}, p_1^{I_2}, q_1^{I_2}$ are suppressed in the matrix elements below when the particular operator for relaxation does not depend on spin, for which the spin indices in the bra and ket parts of the matrix elements are required to be the same. When the matrix elements are given below in the K- and M-symmetrized representations, which are defined later in Eqs. (A36), (A54), and (A56); they are indicated by the subscripts K and KM hereafter.

A.4.1. Isotropic rotational diffusion in liquids (Γ_{iso})

The matrix elements for reorientational motion in isotropic liquids assuming axial symmetry of diffusion motion can be expressed as:

$$\begin{aligned}&\langle L_1 M_1 K_1 | \Gamma_{iso} | L_2 M_2 K_2 \rangle \\ &= \delta_{L_1 L_2} \delta_{M_1 M_2} \delta_{K_1 K_2} \left\{ \begin{array}{l} R_{\perp} L_1(L_1+1)[1+\tau_{\perp} R_{\perp} L_1(L_1+1)]^{-E_{\perp}} \\ +K_1^2 \left[R_{//}(1+\tau_{//} R_{//} K_1^2)^{-E_{//}} - R_{\perp}(1+\tau'_{\perp} R_{\perp} K_1^2)^{-E'_{\perp}} \right] \end{array} \right\}.\end{aligned} \tag{A15}$$

The matrix element for axial symmetry, given by Eq. (A15), is generalized to the non-axial case for Brownian diffusion in the M-symmetrized basis as follows [17]:

$$\begin{aligned}&\langle L_1, M_1, K_1, j_1^K, j_1^M | \Gamma_{\text{iso}} | L_2, M_2, K_2, j_2^K, j_2^M \rangle_{KM} \\ &\quad = \delta_{j_1^M, j_2^M} \delta_{j_1^K, j_2^K} \delta_{L_1, L_2} \delta_{M_1, M_2} \\ &\qquad \times \left[\delta_{K_1, K_2} \left(\frac{R_x + R_y}{2} [L_1(L_1+1) - K_1^2] + R_z K_1^2 \right) \right. \\ &\qquad + (\delta_{K_1 - 2, K_2} N_+(L_1, K_1 - 2) \\ &\qquad \left. + \delta_{K_1+2, K_2} N_-(L_1, K_1 + 2)) N_K(K_1, K_2)^{-1} \frac{(R_x - R_y)}{4} \right],\end{aligned} \tag{A15a}$$

where $N_{\pm}(L,K) = [(L \mp K - 1)(L \mp K)(L \pm K + 1)(L \pm K + 2)]^{1/2}$. (A15b)

For the case of axial diffusion, and treating each degree of freedom independently, the possible limiting situations are taken into account by choosing the following values of the parameters in Eq. (A15):

(a) *Brownian motion.* $\tau = 0$, $E = 0$;
(b) *Free diffusion.* $\tau \neq 0$, $E = 1/2$;
(c) *Jump diffusion.* $\tau \neq 0$, $E = 1$;
(d) *Anisotropic viscosity.* Here one adds the term $(R_{//} - R_{\perp})M_1^2$ in Eqs. (A15) and (A15a)

A.4.2. Rotational diffusion correction in liquid crystals (Γ_U)

For this case, the diffusion operator is given by the symmetrized Smoluchowski equation:

$$\Gamma_{LC} = \left[J - \frac{1}{2k_{\mathrm{B}}T}(JU) \right] R \left[J + \frac{1}{2k_{\mathrm{B}}T}(JU) \right], \tag{A16}$$

where J is the angular momentum operator, U is the mean potential acting on the system, R is the rotational diffusion tensor of the molecule, and k_{B} is the Boltzmann's constant. In terms of U the equilibrium distribution probability is written as

$$P(\Omega) = \exp\{-U/k_{\mathrm{B}}T\} \Big/ \int \mathrm{d}\Omega \exp\{-U/k_{\mathrm{B}}T\}. \tag{A17}$$

The operator Γ_{LC} in Eq. (A16) can be expressed as

$$\Gamma_{LC} = \Gamma_{\text{iso}} + \Gamma_U, \tag{A18}$$

where $\Gamma_{\rm iso}$ is given by Eq. (A15) for $\tau_\perp = \tau'_\perp = \tau_{//} = 0$, and Γ_U is an additional contribution given by

$$\Gamma_U = \frac{1}{2k_BT}\{R_\perp(J^2U) + (R_{//} - R_\perp)(J_z^2U)\} - \frac{1}{4k_B^2T^2}\{R_\perp(J_+U)(J_-U) + R_{//}(J_zU)^2\}. \quad \text{(A19)}$$

The following form is assumed for the orienting potential, assumed to be uniaxial and expanded in terms of spherical harmonics, as follows:

$$U = -k_BT \sum_{L,K}{}' \lambda_k^L D_{0K}^L(\Omega), \quad \text{(A20)}$$

where the prime over summation indicates that the sum is over 0, ±2, ±4 for the indices L and K for convenience as a reasonable approximation, and the expansion coefficients λ_K^L are such that

$$\lambda_K^L = \lambda_{-K}^L = \lambda_K^{L^*}. \quad \text{(A21)}$$

It is noted that the diffusion frame is not axially symmetric when the potential is explicitly dependent on the Euler angle γ in $\Omega(\alpha,\beta,\gamma)$, which happens when some λ_K^L are different from zero for $K \neq 0$, since then a rotation around the z' axis of the frame changes the functional dependence of U on γ. As for the operator Γ_U, it can be written as

$$\Gamma_U = \sum_{L,K} X_L^K D_{0K}^L. \quad \text{(A22)}$$

The coefficients X_K^L in Eq. (A22) are given as follows:

$$X_K^L = X_K^{L'}\delta_{R_x,R_y} + X_K^{L''}(1 - \delta_{R_x,R_y}), \quad \text{(A23)}$$

where $X_K^{L'}$ is the coefficient for the case of axial symmetry ($R_x = R_y = R_\perp$ *and* $R_z = R_{//}$), and $X_K^{L''}$ is the additional coefficient in the absence of axial symmetry ($R_x \neq R_y$ *and* $R_z = R_{//}$). Explicitly [11],

$$X_K^{L'} = -\frac{1}{2}\lambda_K^L\left\{\frac{R_x+R_y}{2}[L(L+1) - K^2] + R_{//}K^2\right\} - \frac{(2L+1)}{4}\sum_{L_1,K_1}\sum_{L_2,K_2}\lambda_{K_1}^{L_1}\lambda_{K_2}^{L_2} \times \begin{pmatrix} L_1 & L & L_2 \\ 0 & 0 & 0 \end{pmatrix}\left\{\begin{array}{l}\left(\frac{R_x+R_y}{2}\right)M_+(L_1,K_1)M_-(L_2,K_2)\begin{pmatrix} L_1 & L & L_2 \\ K_1+1 & -K & K_2-1 \end{pmatrix} \\ +R_{//}K_1K_2\begin{pmatrix} L_1 & L & L_2 \\ K_1 & -K & K_2 \end{pmatrix}\end{array}\right\} \quad \text{(A23a)}$$

and

$$X_K^{L''} = -\frac{1}{2}\frac{(R_x-R_y)}{4} \times \left\{\begin{array}{l}[\lambda_{K+2}^L N_-(L,K+2) + \lambda_{K-2}^L N_+(L,K-2)] + \frac{(2L+1)}{2}\sum_{L_1,K_1}\sum_{L_2,K_2}\lambda_{K_1}^{L_1}\lambda_{K_2}^{L_2}\begin{pmatrix} L_1 & L & L_2 \\ 0 & 0 & 0 \end{pmatrix} \\ \times\left[\begin{array}{l}M_+(L_1,K_1)M_+(L_2,K_2)\begin{pmatrix} L_1 & L & L_2 \\ K_1+1 & -K & K_2+1 \end{pmatrix} \\ +M_-(L_1,K_1)M_-(L_2,K_2)\begin{pmatrix} L_1 & L & L_2 \\ K_1-1 & -K & K_2-1 \end{pmatrix}\end{array}\right]\end{array}\right\}. \quad \text{(A23b)}$$

In Eqs. (A23a) and (A23b):

$$M_+(L_1,K_1) = [L_1(L_1+1) - K_1(K_1+1)]^{1/2};$$
$$M_-(L_2,K_2) = [L_2(L_2+1) - K_2(K_2-1)]^{1/2}.$$

The matrix elements of Γ_U are

$$\langle L_1M_1K_1|\Gamma_U|L_2M_2K_2\rangle = \delta_{M_1,M_2}\sum_L X_{K_1-K_2}^L N_L(L_1,L_2)(-1)^{K_1+M_1} \times \begin{pmatrix} L_1 & L & L_2 \\ M_1 & 0 & -M_1 \end{pmatrix}\begin{pmatrix} L_1 & L & L_2 \\ K_1 & K_2-K_1 & -K_2 \end{pmatrix}. \quad \text{(A24)}$$

In the M-symmetrized representation, the above equation becomes [17]

$$\langle L_1,M_1,K_1,j_1^K,j_1^M|\Gamma_U|L_2,M_2,K_2,j_2^K,j_2^M\rangle_{KM} = \delta_{M_1,M_2}\delta_{j_1^M,j_2^M}\delta_{j_1^K,j_2^K}N_L(L_1,L_2)N_K(K_1,K_2)(-1)^{K_1+M_1} \times \sum_L\begin{pmatrix} L_1 & L & L_2 \\ M_1 & 0 & -M_1 \end{pmatrix}\left[X_{K_1-K_2}^L\begin{pmatrix} L_1 & L & L_2 \\ K_1 & K_2-K_1 & -K_2 \end{pmatrix} + j_2^K(-1)^{L_2+K_2}X_{K_1+K_2}^L\begin{pmatrix} L_1 & L & L_2 \\ K_1 & -K_1-K_2 & K_2 \end{pmatrix}\right]. \quad \text{(A24a)}$$

A.4.3. Discrete jumps among equivalent sites (Γ_{dj})

The matrix elements of this operator independent of electronic and nuclear spins, for the special case that these sites are connected by a rotation around one molecular axis, say the diffusional z'-axis: are [11]:

$$\langle L_1,M_1,K_1|\Gamma_{\rm dj}|L_2,M_2,K_2\rangle = \delta_{L_1,L_2}\delta_{K,K_2}\delta_{M_1,M_2}\frac{1}{\tau_{\rm dj}}(1 - \delta_{K_1}^{n_s}). \quad \text{(A25)}$$

In the M-symmetrized representation, Eq. (A25) becomes [17]:

$$\langle L_1, M_1, K_1, j_1^K, j_1^M | \Gamma_{\mathrm{dj}} | L_2, M_2, K_2, j_2^K, j_2^M \rangle_{KM} = \delta_{L_1,L_2}\delta_{K,K_2}\delta_{M_1,M_2}\delta_{j_1^M,j_2^M}\delta_{j_1^K,j_2^K}\frac{1}{\tau_{\mathrm{dj}}}(1-\delta_{K_1}^{n_s}). \tag{A25a}$$

In Eqs. (A25) and (A25a), τ_{dj} represents the mean distance between jumps, n_s is the number of equivalent sites, and δ_K^n is defined as:

$$\delta_K^n = 1, \quad \text{if } K \text{ is a multiple of } n; = 0, \text{ otherwise.} \tag{A26}$$

A.4.4. Heisenberg spin exchange (Γ_{ex})

Its matrix element, for the case when the lifetime of radical-pair encounters is much shorter than either the time scale associated with the rotational diffusion process (τ_R), and also much shorter than the effective exchange time ($1/\omega_{HE}$), where ω_{HE} is the effective spin-exchange frequency assuming that Γ_{ex} is independent of the orientation of the radical:

$$\langle 01, p_1^{I_1}q_1^{I_1}, p_1^{I_2}q_1^{I_2}; L_1, M_1, K_1, j_1^K, j_1^M | \Gamma_{W_{n1}} + \Gamma_{W_{n1}} | 01, p_2^{I_1}q_2^{I_1}, p_2^{I_2}q_2^{I_2}; L_2, M_2, K_2, j_2^K, j_2^M \rangle_{KM} = \delta_{j_1^M,j_2^M}\delta_{j_1^K,j_2^K}\delta_{L_1,L_2}\delta_{K_1,K_2}\delta_{M_1,M_2} \times \left\{ \begin{array}{l} W_{n1}\delta_{\Delta p^{I_1},0}\delta_{p_1^{I_2},p_2^{I_2}}\delta_{q_1^{I_2},q_2^{I_2}}\left[\begin{array}{l}\delta_{p_1^{I_1},0}\left(\delta_{\Delta q^{I_1},0}(2-\delta_{|q^{I_1}|,2I_1})-\delta_{\Delta q^{I_1},2}\right)\\ +\delta_{|p_1^{I_1}|,1}\left(\frac{13}{6}\delta_{\Delta q^{I_1},0}-\delta_{\Delta q^{I_1},2}\right)+\frac{11}{3}\delta_{|p^{I_1}|,2}\delta_{\Delta q^{I_1},0}\end{array}\right] \\ +W_{n2}\delta_{\Delta p^{I_2},0}\delta_{p_1^{I_1},p_2^{I_1}}\delta_{q_1^{I_1},q_2^{I_1}}\left[\begin{array}{l}\delta_{p_1^{I_2},0}\left(\delta_{\Delta q^{I_2},0}(2-\delta_{|q^{I_2}|,2I_2})-\delta_{\Delta q^{I_2},2}\right)\\ +\delta_{|p_1^{I_2}|,1}\left(\frac{13}{6}\delta_{\Delta q^{I_2},0}-\delta_{\Delta q^{I_2},2}\right)+\frac{11}{3}\delta_{|p^{I_2}|,2}\delta_{\Delta q^{I_2},0}\end{array}\right] \end{array} \right\}, \tag{A27d}$$

$$\langle p_1^s q_1^s, p_1^{I_1}q_1^{I_1}, p_1^{I_2}q_1^{I_2} | \Gamma_{\mathrm{ex}} | p_2^s q_2^s, p_2^{I_1}q_2^{I_1}, p_2^{I_2}q_2^{I_2} \rangle = \omega_{\mathrm{HE}}\delta_{p_1^s p_2^s}\delta_{p_1^{I_1}p_2^{I_1}}\delta_{p_1^{I_2}p_2^{I_2}}\left\{\delta_{q_1^s q_2^s}\delta_{q_1^{I_1},q_2^{I_1}}\delta_{q_1^{I_2}q_2^{I_2}} - \frac{1}{2}\delta_{p_1^s,0}\delta_{q_1^{I_1},q_2^{I_1}}\delta_{q_1^{I_2}q_2^{I_2}} - \frac{1}{(2I_1+1)(2I_2+1)}\delta_{p_1^{I_1},0}\delta_{p_1^{I_2},0}\delta_{q_1^s,q_2^s}\right\}. \tag{A27}$$

The last term in curly brackets in (A27) on the right hand side subtracts off the exchanges for the cases when the electron-nuclear states are the same [20]. In the M-symmetrized representation, Eq. (A27) is generalized, in the model in which spin exchange is considered between molecules of arbitrary orientation, which can yield complete exchange narrowing even for slow-motional spectra, to [17]:

$$\langle p_1^s q_1^s, p_1^{I_1}q_1^{I_1}, p_1^{I_2}q_1^{I_2}; L_1, M_1, K_1, j_1^K, j_1^M | \Gamma_{\mathrm{ex}} | p_2^s q_2^s, p_2^{I_1}q_2^{I_1}, p_2^{I_2}q_2^{I_2}; L_2, M_2, K_2, j_2^K, j_2^M \rangle_{KM} = \omega_{\mathrm{HE}}\delta_{j_1^M,j_2^M}\delta_{j_1^K,j_2^K}\delta_{L_1,L_2}\delta_{K_1,K_2}\delta_{p_1^s p_2^s}\left(\delta_{q_1^{I_1},q_2^{I_1}}\delta_{q_1^{I_2},q_2^{I_2}} - \frac{1}{(2I_1+1)(2I_2+1)}\delta_{p_1^{I_1},0}\delta_{p_1^{I_2},0}\delta_{L_1,0}\right) \times \left[\delta_{p_1^s,0}\tfrac{1}{2}\left(\delta_{M_1,M_2}\delta_{p_1^{I_1}p_2^{I_1}}\delta_{p_1^{I_1},p_2^{I_2}} + j_2^M(-1)^{L_2+M_2}\delta_{M_1,-M_2}\delta_{p_1^{I_1},-p_2^{I_1}}\delta_{p_1^{I_2},-p_2^{I_2}}\right) + \delta_{|p_1^s|,1}\delta_{M_1,M_2}\delta_{p_1^{I_1}p_2^{I_1}}\delta_{p_1^{I_2},p_2^{I_2}}\right]. \tag{A27a}$$

A.4.5. Rotationally independent electron spin flip rate (W_e)

Its contribution is expressed in the M-symmetrized diagonal electronic states as follows [17]:

$$\langle 01, p_1^{I_1}q_1^{I_1}, p_1^{I_2}q_1^{I_2}; L_1, M_1, K_1, j_1^K, j_1^M | \Gamma_{W_e} | 01, p_2^{I_1}q_2^{I_1}, p_2^{I_2}q_2^{I_2}; L_2, M_2, K_2, j_2^K, j_2^M \rangle_{KM} = W_e\delta_{j_1^M,j_2^M}\delta_{j_1^K,j_2^K}\delta_{L_1,L_2}\delta_{K_1,K_2}\delta_{|M_1|,|M_2|}\delta_{|p_1^{I_1}|,|p_2^{I_1}|}\delta_{|p_1^{I_2}|,|p_2^{I_2}|}\delta_{q_1^{I_1},q_2^{I_1}}\delta_{q_1^{I_2},q_2^{I_2}} \times \left(\delta_{p_1^{I_1},p_2^{I_1}}\delta_{p_1^{I_2},p_2^{I_2}}\delta_{M_1,M_2} + j_2^M(-1)^{L_2+M_2}\delta_{p_1^{I_1},-p_2^{I_1}}\delta_{p_1^{I_2},-p_2^{I_2}}\delta_{M_1,-M_2}\right). \tag{A27b}$$

A.4.6. Rotationally-independent nuclear spin-flips (Γ_{Wni}; $i = 1, 2$)

The operator for the additional nuclear spin-flip rates other than that from the rotational motion, has the following matrix element in the M-symmetrized diagonal electronic states [17]:

$$\langle 01, p_1^{I_1}q_1^{I_1}, p_1^{I_2}q_1^{I_2}; L_1, M_1, K_1, j_1^K, j_1^M | \Gamma_{W_{n1}} + \Gamma_{W_{n2}} | 01, p_2^{I_1}q_2^{I_1}, p_2^{I_2}q_2^{I_2}; L_2, M_2, K_2, j_2^K, j_2^M \rangle_{KM} = \delta_{j_1^M,j_2^M}\delta_{j_1^K,j_2^K}\delta_{L_1,L_2}\delta_{K_1,K_2}\delta_{M_1,M_2} \times \left\{ \begin{array}{l} W_{n1}\delta_{\Delta p^{I_1},0}\delta_{p_1^{I_2},p_2^{I_2}}\delta_{q_1^{I_2},q_2^{I_2}}\left[\delta_{p_1^{I_1},0}(\delta_{\Delta q^{I_1},0}-\delta_{\Delta q^{I_1},2})+\frac{7}{6}\delta_{|p_1^{I_1}|,1}\right] \\ +W_{n2}\delta_{\Delta p^{I_2},0}\delta_{p_1^{I_1},p_2^{I_1}}\delta_{q_1^{I_1},q_2^{I_1}}\left[\delta_{p_1^{I_2},0}(\delta_{\Delta q^{I_2},0}-\delta_{\Delta q^{I_2},2})+\frac{7}{6}\delta_{|p_1^{I_2}|,1}\right] \end{array} \right\}, \tag{A27c}$$

for $I_1 = I_2 = 1/2$, and for $I_1 = I_2 = 1$.

For the case when one nucleus has spin 1/2 and the other 1, one should add one term from each of the Eqs. (A27c) and (A27d), appropriately.

A.5. The starting vector

In the context of EPR problems the starting vector in the total spin subspace is defined in terms of the normalized vector associated with $|S_x \otimes 1_1 \otimes 1_2 \otimes P(\Omega)^{1/2}\rangle$ where 1_1 and 1_2 are the unity operators in the nuclear spaces, as in EPR the x_L component of electronic magnetization is measured. As a consequence, its components in the basis set defined by Eqs. (A3) and (A10) are [11]:

$$|v\rangle = 2^{-1/2}(|v_1\rangle + |v_{-1}\rangle) \tag{A28}$$

with

$$\langle p^s q^s; p^{I_1} q^{I_1}; p^{I_2} q^{I_2}; LMK | v_m \rangle = (2I_1+1)^{-1/2}(2I_2+1)^{-1/2}\delta_{p^{I_1},0}\delta_{p^{I_2},0}\delta_{p^s,m}\delta_{M,0} \times \sqrt{\frac{2L+1}{8\pi^2}} \int d\Omega D^{L*}_{0K} P(\Omega)^{1/2}; \quad (m = \pm 1). \tag{A29}$$

The starting vector is expressed in the M-symmetrized basis as [17]:

$$_{KM}\langle p^s q^s; p^{I_1} q^{I_1}; p^{I_2} q^{I_2}; LMK, j^K, j^M | v_m \rangle = \delta_{p^{I_1},0}\delta_{p^{I_2},0}\delta_{p^s,m}\delta_{M,0}\delta_{j^K,1}\delta_{j^M,1}(2I_1+1)^{-1/2} \times (2I_2+1)^{-1/2}\sqrt{\frac{2}{1+\delta_{K,0}}}\sqrt{\frac{2L+1}{8\pi^2}} \times \int d\Omega P(\Omega)^{1/2} \mathrm{Re}\{D^L_{0K}\}; \quad (m = \pm 1). \tag{A29a}$$

In Eqs. (A29) and (A29a) the integral over Ω is non-zero only when L and K are even because of the definition (A20) of U. The probability does not depend on the angle α: $P(\Omega) = P(\beta, \gamma)$. It satisfies the following symmetry properties:

$$P(\beta,\gamma) = P(\beta,-\gamma) = P(\beta,\pi-\gamma) = P(\pi-\beta,\gamma). \tag{A30}$$

A.6. EPR spectrum

The formal expression for the spectrum, given by Eq. (A.1), can be expressed as

$$I(\omega) = \frac{1}{2}\sum_{m,m'} I_{mm'}(\omega); \quad m, m' = \pm 1, \tag{A31}$$

where

$$I_{mm'}(\omega) = \frac{1}{\pi}\mathrm{Re}\langle v_m | [\mathrm{i}(\omega 1 - L) + \Gamma]^{-1} | v_{m'} \rangle. \tag{A32}$$

The number of components of $|v\rangle$ can be decreased in the absence of director tilt ($\psi = 0$) in view of the requirement expressed by Eq. (A13). This is done by making use of the symmetry properties of the matrices involved with respect to the change of sign of the indices $p^s, p^{I_1}, p^{I_2}, K, and\ M$. To this end, one uses the following symmetry property with respect to the change in the signs of the indices corresponding to the various magnetic quantum numbers as exhibited in terms of the matrix $\boldsymbol{Y}$, whose matrix elements are given as

$$\langle p_1^s q_1^s; p_1^{I_1} q_1^{I_1}; p_1^{I_2} q_1^{I_2}; L_1 M_1 K_1 | Y | p_2^s q_2^s; p_2^{I_1} q_2^{I_1}; p_2^{I_2} q_2^{I_2}; L_2 M_2 K_2 \rangle = \delta_{-p_1^s,p_2^s}\delta_{q_1^s,q_2^s}\delta_{-p_1^{I_1},p_2^{I_1}}\delta_{q_1^{I_1},q_2^{I_1}}\delta_{-p_1^{I_2},p_2^{I_2}}\delta_{q_1^{I_2},q_2^{I_2}}\delta_{L_1,L_2}\delta_{-M_1,M_2}\delta_{-K_1,K_2} \times (-1)^{M_1+K_1}. \tag{A33}$$

These matrix elements provide the following properties to Y:

$$Y^2 = 1, \tag{A34a}$$

$$Y|v_m\rangle = |v_{-m}\rangle, \tag{A34b}$$

$$YLY = -L^*, \tag{A34c}$$

$$Y\Gamma Y = \Gamma, \tag{A34d}$$

where Eq. (A34c) is obtained by manipulating Eq. (A12), whereas Eq. (A34d) is obtained by exploiting Eqs. (A15), (A24), (A25), and (A27). It is seen from Eqs. (A34a)–(A34d) that $I_{m,m'}(\omega) = -I_{m,-m'}(-\omega)$.

One can now consider two cases.

A.6.1. EPR spectrum for the case when the director tilt is absent ($\psi = 0°$)

For this case, $I_{-1,1}(\omega) = I_{1,-1}(\omega) = 0$ as a consequence of (A13).The expression for EPR spectrum in this case, as given by Eq. (A31), finally becomes:

$$I(\omega) = \frac{1}{2}[I_{11}(\omega) + I_{11}(-\omega)]. \tag{A35}$$

Thus, according to Eq. (A35), the spectrum can be calculated by using $|v_1\rangle$ as the starting vector, and symmetrizing the spectrum with respect to ω. It is noted that using only the $|v_1\rangle$ part of the starting vector from $|v\rangle$ reduces the size of the matrix to be diagonalized significantly; one can then very efficiently truncate the basis elements with $p^s \neq 1$.

A.6.2. ESR spectrum for the case when the director tilt is arbitrary ($\psi \neq 0$)

In this case, one needs to use the full starting vector $|v\rangle$, as given by Eq. (A28). This is because $I_{-1,1}(\omega) \neq 0$, and the Lanczos algorithm is efficiently applied when the "ket" ($|\mathrm{v}\rangle$) and "bra" ($\langle \mathrm{v}|$) vectors are the same in Eq. (A1).

A.7. Symmetrization of L

A.7.1. K-symmetrization

In order to apply the Lanczo's algorithm, the matrix for $-\boldsymbol{iL}$ in Eq. (A1) required to calculate EPR spectrum should be complex symmetric. To accomplish this, the basis set must be appropriately transformed, so that the operator $\boldsymbol{L}$ has real matrix elements. To this end, one uses the transformed K-symmetrized basis set, indicated by the subscript K hereafter, given as follows:

$$|p^s q^s; p^{I_1} q^{I_1}; p^{I_2} q^{I_2}; L, M, K, j^K\rangle_K = |p^s q^s; p^{I_1} q^{I_1}; p^{I_2} q^{I_2}\rangle \quad \times [2(1+\delta_{K0})]^{-1/2} \times \exp\left\{\mathrm{i}\frac{\pi}{4}(1-j^K)\right\}(|L,M,K\rangle + j^k(-1)^{L+K}|L,M,-K\rangle). \tag{A36}$$

It is noted, for use in Eq. (A36), that

$$\exp\left\{\mathrm{i}\frac{\pi}{4}(1-j^K)\right\} = (j^K)^{1/2}; \quad \text{for } j^K = \pm 1, \tag{A37}$$

where the index K takes only positive values, and the allowed values for j^K are:

$$\begin{aligned} j^K &= \pm 1 \quad \text{if } K > 0, \\ j^K &= (-1)^L \quad \text{if } K = 0. \end{aligned} \tag{A38}$$

Another property exhibited by the j^K value in Eq. (A38) is that it is the eigenvalue, or parity, of the operator $\boldsymbol{C}_2(\boldsymbol{y})$, which performs a π-rotation about the y-axis of the diffusion frame with respect to the eigenvector $|p^s q^s, p^{I_1} q^{I_1}, p^{I_2} q^{I_2} L, M, K, j^K\rangle_K$ as follows:

$$\begin{aligned} &C_{2(y)} |p^s q^s p^{I_1} q^{I_1} p^{I_2} q^{I_2}; L, M, K, j^K\rangle_K \\ &\quad = j^K |p^s q^s p^{I_1} q^{I_1} p^{I_2} q^{I_2}; L, M, K, j^K\rangle_K. \end{aligned} \tag{A38a}$$

Eq. (A38a) is a consequence of a fundamental symmetry of the basis set, specifically, the parity of the basis kets with respect to the $\boldsymbol{C}_2$ ($\boldsymbol{y}$) operator:

$$C_{2(y)} |L, M, K\rangle = (-1)^{L+K} |L, M, -K\rangle,$$

which leads to Eq. (A38a) by the use of Eq. (A36).

Finally, it is noted that in order to convert the SLO to a complex symmetric form, one needs an additional factor of i for the basis vectors with $j^K = -1$, which is already built into Eq. (A36).

The elements of the starting vector $|v_m\rangle$ in the K-representation is as follows:

$$\begin{aligned} &{}_K\langle p^s q^s; p^{I_1} q^{I_1}; p^{I_2} q^{I_2}; L, M, K, j^K | v_m \rangle \\ &\quad = \delta_{m,p^s} \delta_{0,p^{I_1}} \delta_{0,p^{I_2}} \delta_{0,M} \delta_{1,j^K} (2I_1 + 1)^{-1/2} \\ &\qquad \times (2I_2 + 1)^{-1/2} \left[\frac{2}{(1 + \delta_{K0})} \right]^{1/2} \sqrt{\frac{2L+1}{8\pi^2}} \\ &\qquad \times \int \mathrm{d}\Omega P(\Omega)^{1/2} \mathrm{Re}\{D^L_{0K}\}. \end{aligned} \tag{A39}$$

In the M-symmetrized basis, the elements of the starting vector are expressed as [17]:

$$\begin{aligned} &{}_{KM}\langle p^s q^s; p^{I_1} q^{I_1}; p^{I_2} q^{I_2}; LMK, j^K, j^M | v_m \rangle \\ &\quad = \delta_{m,p^s} \delta_{0,p^{I_1}} \delta_{0,p^{I_2}} \delta_{0,M} \delta_{1,j^K} \delta_{1,j^M} (2I_1 + 1)^{-1/2} \\ &\qquad \times (2I_2 + 1)^{-1/2} \left[\frac{2}{(1 + \delta_{K0})} \right]^{1/2} \sqrt{\frac{2L+1}{8\pi^2}} \\ &\qquad \times \int \mathrm{d}\Omega P(\Omega)^{1/2} \mathrm{Re}\{D^L_{0K}\}. \end{aligned} \tag{A39a}$$

The matrix elements of the operators Γ_U and $L(=H^\times)$ in the K- and M-symmetrized *off-diagonal* ($p^s_1 = p^s_2 = \pm 1$; $q^s_1 = q^s_2 = 0$) and M-symmetrized *diagonal* ($p^s_1 = p^s_2 = 0$; $q^s_1 = q^s_2 = 1$) bases are as follows [11,17]:

$$\begin{aligned} &\langle p^s q^s p^{I_1} q^{I_1} p^{I_2} q^{I_2} L_1 M_1 K_1 j^K_1 | \Gamma_U | p^s q^s p^{I_1} q^{I_1} p^{I_2} q^{I_2} L_2 M_2 K_2 j^K_2 \rangle_K \\ &\quad = \delta_{M_1,M_2} \delta_{j^K_1, j^K_2} N_L(L_1, L_2) N_K(K_1, K_2) (-1)^{L_1 + M_1} \\ &\qquad \times \sum_L \begin{pmatrix} L_1 & L & L_2 \\ M_1 & 0 & -M_1 \end{pmatrix} \left\{ \begin{aligned} &X^L_{K_1 - K_2} \begin{pmatrix} L_1 & L & L_2 \\ K_1 & K_2 - K_1 & -K_2 \end{pmatrix} \\ &+ j^K_2 (-1)^{L_2 + K_2} X^L_{K_1 + K_2} \begin{pmatrix} L_1 & L & L_2 \\ K_1 & -K_1 - K_2 & K_2 \end{pmatrix} \end{aligned} \right\}, \end{aligned} \tag{A40}$$

$$\begin{aligned} &\langle p^s q^s p^{I_1} q^{I_1} p^{I_2} q^{I2} L_1 M_1 K_1 j^K_1 j^M_1 | \Gamma_U | p^s q^s p^{I_1} q^{I_1} p^{I_2} q^{I2} L_2 M_2 K_2 j^K_2 j^M_2 \rangle_{KM} \\ &\quad = \delta_{M_1,M_2} \delta_{j^K_1, j^K_2} \delta_{j^M_1, j^M_2} N_L(L_1, L_2) N_K(K_1, K_2) (-1)^{M_1 + K_1} \\ &\qquad \times \sum_L \begin{pmatrix} L_1 & L & L_2 \\ M_1 & 0 & -M_1 \end{pmatrix} \left\{ \begin{aligned} &X^L_{K_1 - K_2} \begin{pmatrix} L_1 & L & L_2 \\ K_1 & K_2 - K_1 & -K_2 \end{pmatrix} \\ &+ j^K_2 (-1)^{L_2 + K_2} X^L_{K_1 + K_2} \begin{pmatrix} L_1 & L & L_2 \\ K_1 & -K_1 - K_2 & K_2 \end{pmatrix} \end{aligned} \right\}, \end{aligned} \tag{A40a}$$

$$\begin{aligned} &\langle p^s_1 q^s_1; p^{I_1}_1 q^{I_1}_1; p^{I_2}_1 q^{I_2}_1; L_1 M_1 K_1, j^K_1 | L | p^s_2 q^s_2; p^{I_1}_2 q^{I_1}_2; p^{I_2}_2 q^{I_2}_2; L_2 M_2 K_2, j^K_2 \rangle_K \\ &\quad = N_L(L_1, L_2) N_K(K_1, K_2) (-1)^{M_1 + K_1} \\ &\qquad \times \sum_{\mu(=g, A_1, A_2), \ell} \left\{ \begin{aligned} &\langle p^s_1 q^s_1; p^{I_1}_1 q^{I_1}_1; p^{I_2}_1 q^{I_2}_1 | [A^{(\ell, \Delta p)^\times}_{\mu, L}] | p^s_2 q^s_2; p^{I_1}_2 q^{I_1}_2; p^{I_2}_2 q^{I_2}_2 \rangle \\ &\quad \times d^\ell_{\Delta p, M_1 - M_2}(\psi) \begin{pmatrix} L_1 & \ell & L_2 \\ M_1 & M_2 - M_1 & -M_2 \end{pmatrix} R_{\mu,\ell}(L_1, K_1, j^K_1; L_2, K_2, j^K_2) \end{aligned} \right\} \\ &\qquad + \delta_{j^K_1 j^K_2} \delta_{p^s_1 p^s_2} \delta_{q^s_1 q^s_2}, \delta_{p^{I_1}_1 p^{I_1}_2} \delta_{q^{I_1}_1 q^{I_1}_2} \delta_{p^{I_2}_1 p^{I_2}_2} \delta_{q^{I_2}_1 q^{I_2}_2} \delta_{L_1 L_2} \delta_{M_1 M_2} \delta_{K_1 K_2} \\ &\qquad \times \frac{\beta_N B}{\hbar} (g_{N_1} p^{I_1}_1 + g_{N_2} p^{I_2}_1), \end{aligned} \tag{A41}$$

$$\begin{aligned}
&\langle \pm 10; p_1^{I_1} q_1^{I_1}; p_1^{I_2} q_1^{I_2}; L_1 M_1 K_1, j_1^K, j_1^M | L | \pm 10; p_2^{I_1} q_2^{I_1}; p_2^{I_2} q_2^{I_2}; L_2 M_2 K_2, j_2^K, j_2^M \rangle_{KM} \\
&\quad = N_L(L_1, L_2) N_K(K_1, K_2) N_p(p_1^{I_1}, p_1^{I_2}, M_1; p_2^{I_1}, p_2^{I_2}, M_2)(-1)^{M_1+K_1} \\
&\quad \times \left[\begin{array}{l} \left\{ \begin{array}{l} \delta_{j_1^M j_2^M} \sum\limits_{\mu(=g,A_1,A_2),\ell} R_{\mu,\ell}(L_1, K_1, j_1^K; L_2, K_2, j_2^K) \\ \quad \times \langle \pm 10; p_1^{I_1} q_1^{I_1}; p_1^{I_2} q_1^{I_2} | [A_{\mu,L}^{(\ell,\Delta p)^\times}] | \pm 10; p_2^{I_1} q_2^{I_1}; p_2^{I_2} q_2^{I_2} \rangle d^\ell_{\Delta p, M_1 - M_2}(\psi) \begin{pmatrix} L_1 & \ell & L_2 \\ M_1 & M_2 - M_1 & -M_2 \end{pmatrix} \\ \quad + j_2^M (-1)^{L_2+M_2} \langle \pm 10; p_1^{I_1} q_1^{I_1}; p_1^{I_2} q_1^{I_2} | [A_{\mu,L}^{(\ell, p_1^{I_1}+p_2^{I_1}+p_1^{I_2}+p_2^{I_2})^\times}] | \pm 10; p_2^{I_1} q_2^{I_1}; p_2^{I_2} q_2^{I_2} \rangle \\ \quad \times d^\ell_{p_1^{I_1}+p_2^{I_1}+p_1^{I_2}+p_2^{I_2}, M_1+M_2}(\psi) \begin{pmatrix} L_1 & \ell & L_2 \\ M_1 & -M_1 - M_2 & M_2 \end{pmatrix} \end{array} \right\} \\ + (1 - \delta_{j_1^M j_2^M}) \delta_{j_1^K j_2^K} \delta_{p_1^s p_2^s} \delta_{q_1^s q_2^s} \delta_{p_1^{I_1} p_2^{I_1}} \delta_{q_1^{I_1} q_2^{I_1}} \delta_{p_1^{I_2} p_2^{I_2}} \delta_{q_1^{I_2} q_2^{I_2}} \delta_{L_1 L_2} \delta_{M_1 M_2} \delta_{K_1 K_2} \\ \quad \times \frac{\beta_N B}{\hbar} (g_{N_1} p_1^{I_1} + g_{N_2} p_1^{I_2}) \end{array} \right]
\end{aligned} \tag{A41a}$$

$$\begin{aligned}
&\langle 01; p_1^{I_1} q_1^{I_1}; p_1^{I_2} q_1^{I_2}; L_1 M_1 K_1, j_1^K, j_1^M | L | 01; p_2^{I_1} q_2^{I_1}; p_2^{I_2} q_2^{I_2}; L_2 M_2 K_2, j_2^K, j_2^M \rangle_{KM} \\
&\quad = N_L(L_1, L_2) N_K(K_1, K_2)(-1)^{M_1+K_1} \\
&\quad \times \left[\begin{array}{l} \delta_{j_1^M j_2^M} \sum\limits_{\mu(=g,A_1,A_2),\ell} R_{\mu,\ell}(L_1, K_1, j_1^K; L_2, K_2, j_2^K) \\ \quad \times \langle 01; p_1^{I_1} q_1^{I_1}; p_1^{I_2} q_1^{I_2} | [A_{\mu,L}^{(\ell,\Delta p^I)^\times}] | 01; p_2^{I_1} q_2^{I_1}; p_2^{I_2} q_2^{I_2} \rangle d^\ell_{\Delta p^I, M_1 - M_2}(\psi) \begin{pmatrix} L_1 & \ell & L_2 \\ M_1 & M_2 - M_1 & -M_2 \end{pmatrix} \\ \quad + (1 - \delta_{j_1^M j_2^M}) \delta_{j_1^K j_2^K} \delta_{p_1^s p_2^s} \delta_{q_1^s q_2^s} \delta_{p_1^{I_1} p_2^{I_1}} \delta_{q_1^{I_1} q_2^{I_1}} \delta_{p_1^{I_2} p_2^{I_2}} \delta_{q_1^{I_2} q_2^{I_2}} \delta_{L_1 L_2} \delta_{M_1 M_2} \delta_{K_1 K_2} \\ \quad \times \frac{\beta_N B}{\hbar} (g_{N_1} p_1^{I_1} + g_{N_2} p_1^{I_2}) \end{array} \right]
\end{aligned} \tag{A42}$$

It is noted that there is present no term in Eq. (A42) in place of $[A_{\mu,\ell}^{\ell, p_1^{I_1}+p_2^{I_1}+p_1^{I_2}+p_2^{I_2}}]^\times$ for the diagonal space, corresponding to the second matrix element in Eq. (A41a) in the off-diagonal space. This is because

$$\begin{aligned}
&\langle 0, 1, p_1^{I_1}, q_1^{I_1}, p_1^{I_2}, q_1^{I_2} | [A_{\mu,\ell}^{\ell, p_1^{I_1}+p_2^{I_1}+p_1^{I_2}+p_2^{I_2}}]^\times | 0, 1, p_2^{I_1}, q_2^{I_1}, p_2^{I_2}, q_2^{I_2} \rangle \\
&\quad = 0
\end{aligned}$$

in the original basis for all interactions as seen from Appendix C.

In Eqs. (A41a) and (A42), $N_L(L_1,L_2)$ and Δp are given by Eq. (A11a), and

$$\Delta p^I = p_1^{I_1} + p_1^{I_2} - p_2^{I_1} - p_2^{I_2}; \tag{A42a}$$

$$N_K(K_1, K_2) = (1 + \delta_{K_1,0})^{-1/2} (1 + \delta_{K_2,0})^{-1/2}; \tag{A42b}$$

$$\begin{aligned}
&N_p(p_1^{I_1}, p_1^{I_2}, M_1; p_2^{I_1}, p_2^{I_2}, M_2) \\
&\quad = \left[(1 + \delta_{p_1^{I_1},0} \delta_{p_1^{I_2},0} \delta_{M_1,0})(1 + \delta_{p_2^{I_1},0} \delta_{p_2^{I_2},0} \delta_{M_2,0}) \right]^{-1/2};
\end{aligned} \tag{A42c}$$

$$\begin{aligned}
R_{\mu,\ell}(L_1 K_1 j_1^K; L_2 K_2 j_2^K) &= \begin{pmatrix} L_1 & \ell & L_2 \\ K_1 & K_2 - K_1 & -K_2 \end{pmatrix} G_{\mu,\ell}(j_1^K, j_2^K, K_1 - K_2) \\
&\quad + j_2^K (-1)^{L_2+K_2} \begin{pmatrix} L_1 & \ell & L_2 \\ K_1 & -K_1 - K_2 & K_2 \end{pmatrix} G_{\mu,\ell}(j_1^K, j_2^K, K_1 + K_2),
\end{aligned} \tag{A43}$$

with

$$G_{\mu,\ell}(j_1^K, j_2^K; K) = \delta_{j_1^K, j_2^K} \mathrm{Re}\{F_{\mu,D}^{(\ell,k)}\} + (1 - \delta_{j_1^K, j_2^K}) j_1^K \mathrm{Im}\{F_{\mu,D}^{(\ell,k)}\}. \tag{A44}$$

In Eq. (A44), the spherical components $F_{\mu,D}^{(\ell,k)}$ can be calculated by transforming directly from the laboratory frame, in which the elements of the $\boldsymbol{g}$, $\boldsymbol{A}_1$, and $\boldsymbol{A}_2$ matrices have been determined, which is, in general, not coincident with any of the principal-axes frames of the various magnetic tensors, to the diffusion (D) frame, as done in the present case. This avoids the extra effort to diagonalize the $\boldsymbol{g}$, $\boldsymbol{A}_1$, and $\boldsymbol{A}_2$ matrices in the procedure described in [11]. To this end, one uses the following transformation:

$$F_{\mu,D}^{(\ell,k)*} = \sum_m D_{k,m}^\ell(\Omega_{D\to L}) F_{\mu,L}^{(\ell,m)*}. \tag{A45}$$

On the other hand, one can, indeed, use the principal values of the $\boldsymbol{g}$, $\boldsymbol{A}_1$, $\boldsymbol{A}_2$ matrices, as done in [11], using the transformations given by Eq. (A8), to express $F_{\mu,D}^{(\ell,k)}$ required in Eq. (A44) as follows:

$$F_{g,D}^{(\ell,k)*} = \sum_m D_{k,m}^\ell(\Omega_{D\to g}) F_{g,g}^{(\ell,m)*}, \tag{A46a}$$

$$\begin{aligned}
F_{A_i,D}^{(\ell,k)*} &= \sum_m D_{k,m}^\ell(\Omega_{D\to A_i}) F_{A_i,A}^{(\ell,m)*} \\
&= \sum_{m,m'} D_{k,m}^\ell(\Omega_{D\to g}) D_{m,m'}^\ell(\Omega_{g\to A_i}) F_{A_i,A}^{(\ell,m')*} \quad (i = 1, 2).
\end{aligned} \tag{A46b}$$

A.8. Symmetries of the EPR problem

The sizes of the matrices can be reduced using the specific symmetries of an ESR problem. In particular, the following cases are considered.

(i) Absence of director tilt ($\psi = 0$).In accordance with (A13), here one only needs the basis elements with

$$M = p^s + p^{I_1} + p^{I_2} - 1. \tag{A47}$$

(ii) $Im(F^{(2,k)}_{\mu,D}) = 0$. In this case, only the basis elements with $j^K = 1$ are required. This happens when the g and the two A matrices have the same principal axes, and the molecular tilt is defined only by the polar angle:

$$\Omega_{D\to g} = \Omega_{D\to A_i}(0,\beta,0); \quad i = 1,2. \tag{A48}$$

(iii) $F^{(2,\pm1)}_{\mu,D} = 0$. Here only the even values of the index K are required. This is the case when there exists no molecular tilt.

(iv) $F^{(2,m)}_{\mu,D} = \delta_{m,0}$. For this case only the basis elements with even L and $K = 0$, are required. This happens when there exists no molecular tilt and the g and A matrices possess axial symmetry.

A.9. The high-field case: matrix elements

In this case, the following conditions hold true:

$$\begin{aligned} &|\omega - \omega_0| \ll \omega_0, \\ &|A_{jj}| \ll g_0\mu_B B_0, \\ &|g_{jj} - \bar{g}| \gg \bar{g}, \end{aligned} \tag{A49}$$

where $\omega_0 = \bar{g}\mu_B B_0/\hbar$, and g_0 have been defined in Section 3 following Eq. (1).

The effect of the non-secular terms, which contain the operators S_+ and S_- in the hyperfine part of the spin Hamiltonian, is taken here into account by perturbation using Van-Vleck formalism [11]. Accordingly, one obtains the following expression for the absorption function:

$$I(\omega) = \frac{1}{\pi}\mathrm{Re}\{\langle v_p|[\mathrm{i}(\omega 1 - L_p) + \Gamma_p]^{-1}|v_p\rangle\}, \tag{A50}$$

where, for the allowed EPR transitions $m^{s'} = 1/2 \leftrightarrow m^{s''} = -1/2$, one is confined to the subspace defined by $p^s = 1, q^s = 0$. Then, the vector $|v_p\rangle$ and the matrix Γ_p are, respectively, the vector $|v_1\rangle$ and the matrix Γ with the elements calculated in this subspace. The matrix L_p is defined as follows:

$$L_p = L' + \frac{1}{\omega_0}\sum_m L''_m (L''_m)^{\mathrm{tr}}; \quad m = \pm 1, \tag{A51}$$

where L' is the submatrix obtained from L for $p^s_1 = p^s_2 = 1$; $q^s_1 = q^s_2 = 0$; L''_m is the submatrix obtained for L for $p^s_1 = 1$, $p^s_2 = 0$; $q^s_1 = 0$, $q^s_2 = m$; and tr indicates the transposed matrix.

For high fields and for motions that are not extremely fast the contributions of the non-secular terms in the spin Hamiltonian can be ignored. This results in the decoupling of the three spin spaces. It is then possible to take advantage of the additional symmetries in both the diagonal and off-diagonal subspaces. One can thus conveniently use the symmetry of the untransformed Liouville submatrix L', and transform the basis elements appropriately using Eqs. (C7) and (C9) of Appendix C, as follows [11]:

$$\begin{aligned} &\langle 1,0;-p^{I_1}_1,q^{I_1}_1;-p^{I_2}_1,q^{I_2}_1|[A^{(\ell,-m)}_\mu]^\times|1,0;-p^{I_1}_2,q^{I_1}_2;-p^{I_2}_2,q^{I_2}_2\rangle \\ &\quad = (-1)^{(p^{I_1}_1+p^{I_2}_1+p^{I_1}_2+p^{I_2}_2)}\langle 1,0;p^{I_1}_1,q^{I_1}_1;p^{I_2}_1,q^{I_2}_1|[A^{(\ell,m)}_\mu]^\times \\ &\quad\quad |1,0;p^{I_1}_2,q^{I_1}_2;p^{I_2}_2,q^{I_2}_2\rangle. \end{aligned} \tag{A52}$$

This result can now be substituted into Eq. (A41) to obtain [11]:

$$\begin{aligned} &\langle 1,0;-p^{I_1}_1,q^{I_1}_1;-p^{I_2}_1,q^{I_2}_1;L_1,-M_1,K_1,j^K_1|L'|1,0;-p^{I_1}_2,q^{I_1}_2; \\ &\quad -p^{I_2}_2,q^{I_2}_2;L_2,-M_2,K_2,j^K_2\rangle_K = (-1)^{L_1+L_2+M_1+M_2} \\ &\quad \langle 1,0;p^{I_1}_1,q^{I_1}_1;p^{I_2}_1,q^{I_2}_1;L_1,M_1,K_1,j^K_1|L'|1,0;p^{I_1}_2, \\ &\quad q^{I_1}_2;p^{I_2}_2,q^{I_2}_2;L_2,M_2,K_2,j^K_2\rangle_K \end{aligned} \tag{A53}$$

and a similar equation can be derived for $\mathbf{\Gamma}_p$.

The above discussion leads to further symmetrization of the K-symmetrized basis as described below.

A.10. M-symmetrized basis

By examining the symmetry properties described by Eqs. (A52) and (A53), one may use transformed basis sets in the off-diagonal and diagonal electronic subspaces in which the elements of Γ and L' are defined as follows [17].

A.10.1. Off-diagonal electronic subspace

For this case, the M-symmetrized basis is described as

$$\begin{aligned} &|\pm 1,0;p^{I_1},q^{I_1};p^{I_2},q^{I_2};L,M,K,j^M,j^K\rangle_{KM} \\ &\quad = [2(1+\delta_{M,0}\delta_{p^{I_1},0}\delta_{p^{I_2},0})]^{-1} \\ &\quad\quad (|\pm 1,0;p^{I_1},q^{I_1};p^{I_2},q^{I_2};L,M,K,j^K\rangle_K + j^M(-1)^{L+M} \\ &\quad\quad |\pm 1,0;-p^{I_1},q^{I_1};-p^{I_2},q^{I_2};L,-M,K,j^K\rangle_K). \end{aligned} \tag{A54}$$

In this new basis, one uses only positive values for the index M and the index j^M is allowed to have only the following values:

$$\begin{aligned} j^M &= (-1)^L, \quad \text{when } p^{I_1} = p^{I_2} = M = 0; \\ &= \pm 1, \quad \text{otherwise. (That is one uses both the basis sets constructed with } j^M = \pm 1). \end{aligned} \tag{A55}$$

It is noted now that the operator Γ_p is factored with respect to j^M in the new off-diagonal basis set, and its

matrix elements are given in Eq. (A41a). The starting vector $|v_m\rangle$ has components only for $j^M = 1$, and they are given in Eq. (A39a). (For this reason, in [15] j^M is not at all used as only the diagonal operator L' is used there).

A.10.2. Diagonal electronic subspace

The M-symmetrization in the diagonal subspace can be expressed as [17]

$$\langle \pm 1,0;p_1^{I_1},q_1^{I_1};p_1^{I_2},q_1^{I_2}|L_1M_1K_1j_1^Mj_1^K|L''_M|0,m;p_2^{I_1},q_2^{I_1};p_2^{I_2},q_2^{I_2};L_2M_2K_2j_2^Mj_2^K\rangle = A\times\sum_{\mu,\ell}B_{\mu,\ell}\times R_{\mu,\ell}(L_1K_1j_1^K;L_2K_2j_2^K),\quad (m=\pm1), \tag{A57}$$

where

$$A = N_L(L_1,L_2)N_K(K_1,K_2)\times[2(1+\delta_{M_1,0}\delta_{p_1^{I_1},0}\delta_{p_1^{I_2},0})]^{-1/2}(-1)^{M_1+K_1} \tag{A57a}$$

and

$$B_{\mu,\ell} = \left\{ \begin{array}{l} \langle \pm1,0;p_1^{I_1},q_1^{I_1};p_1^{I_2},q_1^{I_2}|[A_\mu^{(\ell,1+p_1^{I_1}-p_2^{I_1}+p_2^{I_1}-p_2^{I_2})}]^\times|0,m;p_2^{I_1},q_2^{I_1};p_2^{I_2},q_2^{I_2}\rangle \\ \quad\times d^\ell_{1+p_1^{I_1}-p_2^{I_1}+p_2^{I_1}-p_2^{I_2},M_1-M_2}(\psi)\begin{pmatrix} L_1 & \ell & L_2 \\ M_1 & M_2-M_1 & -M_2\end{pmatrix} \\ \quad+j_1^M(-1)^{L_1+M_1} \\ \quad\times\langle \pm1,0;-p_1^{I_1},q_1^{I_1};-p_1^{I_2},q_1^{I_2}|[A_\mu^{(\ell,1-p_1^{I_1}-p_2^{I_1}-p_1^{I_2}-p_2^{I_2})}]^\times|0,m;p_2^{I_1},q_2^{I_1};p_2^{I_2},q_2^{I_2}\rangle \\ \quad\times d^\ell_{1-p_1^{I_1}-p_1^{I_2}-p_2^{I_1}-p_2^{I_2},-M_1-M_2}(\psi)\times\begin{pmatrix} L_1 & \ell & L_2 \\ -M_1 & M_2+M_1 & -M_2\end{pmatrix} \end{array} \right\} \tag{A57b}$$

$$|0,1;p^{I_1},q^{I_1};p^{I_2},q^{I_2};L,M,K,j^M,j^K\rangle_{KM} = \tfrac{1}{\sqrt{2}}\begin{pmatrix} |0,1;p^{I_1},q^{I_1};p^{I_2},q^{I_2};L,M,K,j^K\rangle_K \\ -j^M(-1)^{L+M}|0,-1;-p^{I_1},q^{I_1};-p^{I_2},q^{I_2};L,-M,K,j^K\rangle_K\end{pmatrix}, \tag{A56}$$

The differences between this basis and the basis in the off-diagonal subspace are as follows: (i) Here the linear combinations are made with respect to q^s, in addition to those with respect to M, p^{I_1}, and p^{I_2}; (ii) The index $j^M = \pm1$ *regardless* of the other indices; (iii) The index M after the symmetrization *may* take a negative number. In any case, Eq. (A56) will still be referred to as M-symmetrization as it has a very close relationship to the M-symmetrization in the off-diagonal electronic subspace.

It is noted that the basis vectors on the right hand side of Eq. (A56) represent the population of the spin states with $m_{I_1} = q^{I_1}/2$; $m_{I_2} = q^{I_2}/2$ and $m_S = \pm1/2$. In that case, the difference between the populations corresponding to the two basis vectors with $q^S = \pm1$ is proportional to the electronic polarization with the characteristic relaxation time, T_1. The sum of these two populations, which is the total population, of course, remains conserved in the absence of cross relaxations involving the nuclear states.

The matrix elements of the Liouville operator for the M-symmetrized basis in the diagonal space have been given in Eq. (A42).

A.11. Matrix elements of the perturbation L''

The operator L'' is defined in Eq. (A51), and its matrix elements are non-zero only between the *diagonal*, $|0,m\rangle$, and the *off–diagonal*, $|\pm1,0\rangle$ electronic subspaces. They are given as [7]:

and $R_{\mu,\ell}(L_1K_1j_1^K;L_2K_2j_2^K)$ is given in Eq. (A43).

Finally it is noted that if the perturbation contributions, determined by the matrix L'' in Eq. (A51), were not considered, the matrix for the relaxation superoperator $\Gamma_p - iL_p$ would be factored with respect to the index j^M. In that case, only the submatrix confined to the diagonal subspace $j_1^M = j_2^M = 1$ needs to be considered as done in [15], where the index j^M has been dropped altogether for this reason.

Appendix B. Spin Hamiltonian

The spin Hamiltonian as given by Eq. (A7) is expressed in the laboratory frame by choosing the index $\eta = L$. A complete listing of the following coefficients:

$$g^{(0,0)}, F_{g,L}^{(0,0)}; g^{(2,p)}, F_{g,L}^{(2,p)} \quad \text{and } F_{A,L}^{(2,p)}\ (p=\pm2,\pm1,0),$$

to be used in Eq. (A7) is given here. These include the off-diagonal elements of the matrices $\boldsymbol{g}$, $\boldsymbol{A}_1$, and $\boldsymbol{A}_2$. It is noted that in [15], irreducible spherical tensor operators (ISTO) for $g^{(2,\pm1)}$, $F_{g,L}^{(2,\pm1)}$, and $F_{A,L}^{(2,\pm1)}$, as well as the terms depending on the off-diagonal elements of the $\boldsymbol{g}$ and $\boldsymbol{A}$ matrices required in $g^{(2,\pm2)}$, $F_{g,L}^{(2,\pm2)}$, and $F_{A,L}^{(2,\pm2)}$, were not listed, because of the use of the coincident principal-axes frames of the $\boldsymbol{g}$ and $\boldsymbol{A}$ matrices in [15]. These are listed here, since the $\boldsymbol{g}$ and the two $\boldsymbol{A}$ matrices are not coincident with each other; thus the experimentally determined values of the $\boldsymbol{g}$ and the two $\boldsymbol{A}$ matrices contain non-zero off-diagonal elements, which were not taken into account in [15].

$$
\begin{aligned}
g^{(0,0)} &= -\sqrt{\frac{1}{3}}(g_{xx}+g_{yy}+g_{zz}) \\
g^{(2,0)} &= \sqrt{\frac{2}{3}}\left(g_{zz}-\frac{1}{2}[g_{xx}+g_{yy}]\right) \\
g^{(2,\pm1)} &= \mp\frac{1}{2}[(g_{xz}+g_{zx}) \pm i(g_{yz}+g_{zy})] \\
g^{(2,\pm2)} &= \frac{1}{2}[(g_{xx}-g_{yy}) \pm i(g_{xy}+g_{yx})]
\end{aligned}
\tag{B1}
$$

$$
\begin{aligned}
F^{o,0}_{g,g} &= -\sqrt{\frac{1}{3}}\left(\frac{\mu_B}{\hbar}\right)[g_{xx}+g_{yy}+g_{yy}] \\
F^{2,0}_{g,g} &= \left(\frac{\mu_B}{\hbar}\right)g^{(2,0)} \\
F^{2,\pm1}_{g,g} &= \mp\frac{1}{2}\left(\frac{\mu_B}{\hbar}\right)[(g_{xz}+g_{zx}) \pm i(g_{yz}+g_{zy})] \\
F^{2,\pm2}_{g,g} &= \frac{1}{2}\left(\frac{\mu_B}{\hbar}\right)[(g_{xx}-g_{yy}) \pm i(g_{xy}+g_{yx})]
\end{aligned}
\tag{B2}
$$

$$
\begin{aligned}
F^{0,0}_{a,ai} &= -\sqrt{\frac{1}{3}}\left(\frac{g_e\mu_B}{\hbar}\right)[(A_{ixx}+A_{iyy}+A_{izz}] \\
F^{2,0}_{a,ai} &= \sqrt{\frac{2}{3}}\left(\frac{g_e\mu_B}{\hbar}\right)\left[A_{izz}-\frac{1}{2}(A_{ixx}+A_{iyy})\right]; \quad i=1,2 \\
F^{2,\pm1}_{a,ai} &= \mp\frac{1}{2}\left(\frac{g_e\mu_B}{\hbar}\right)[(A_{ixz}+A_{izx}) \pm i(A_{iyz}+A_{izy})] \\
F^{2,\pm2}_{a,ai} &= \frac{1}{2}\left(\frac{g_e\mu_B}{\hbar}\right)[(A_{ixx}-A_{iyy}) \pm i(A_{ixy}+A_{iyx})]
\end{aligned}
\tag{B3}
$$

As for the coupling of rank-one operators associated with the electron spin ($\boldsymbol{S}$) and the magnetic-field vector ($\boldsymbol{B}$), they are listed below for the general case when all the components of $\boldsymbol{B}$ are non-zero for completeness:

$$
\begin{aligned}
A^{(0,0)}_{g,L} &= -\left(\frac{1}{\sqrt{3}}\right)(B_zS_z+B_xS_x+B_yS_y) \\
A^{(2,0)}_{g,L} &= \left(\frac{1}{\sqrt{6}}\right)[3B_zS_z-(B_xS_x+B_yS_y+B_zS_z)] \\
A^{(2,\pm1)}_{g,L} &= \mp\left(\frac{1}{2}\right)(B_zS_\pm+S_zB_\pm) \\
A^{(2,\pm2)}_{g,L} &= \left(\frac{1}{2}\right)B_\pm S_\pm.
\end{aligned}
\tag{B4}
$$

In Eqs. (B4), $B_\pm = B_x \pm \mathrm{i}B_y$ and $S_\pm = S_x \pm \mathrm{i}S_y$.

The corresponding expressions for coupling between the electronic and nuclear spins become:

$$
\begin{aligned}
A^{(0,0)}_{ai,L} &= -\left(\frac{1}{\sqrt{3}}\right)(I_{iz}S_z+I_{ix}S_x+I_{iy}S_y); \quad i=1,2 \\
A^{(2,0)}_{ai,L} &= \left(\frac{1}{\sqrt{6}}\right)[3I_{iz}S_z-(I_{ix}S_x+I_{iy}S_y+I_{iz}S_z)]; \quad i=1,2 \\
A^{(2,\pm1)}_{ai,L} &= \mp\left(\frac{1}{2}\right)(I_{iz}S_\pm+S_zI_{i\pm}); \quad i=1,2 \\
A^{(2,\pm2)}_{ai,L} &= \left(\frac{1}{2}\right)I_{i\pm}S_\pm; \quad i=1,2
\end{aligned}
\tag{B5}
$$

For the isotropic nuclear Zeeman term, one has

$$
F^{0,0}_{n,ni} = -\frac{g_{Ni}\mu_N}{\hbar}, \quad A^{0,0}_{ni,L} = BI_{iz}; \quad i=1,2 \tag{B6}
$$

Appendix C. Matrix elements of $[A^{(\ell,m)}_{\mu}]^{\times}$

This appendix deals with the extension of the matrix elements given in [7] to the case of one electron spin coupled to two nuclear spins. (Every effort is made here to correct for the numerous typos in [11].)

It is first noted that the Liouville operator $A^{\times}$ associated with the operator A, which can be either a nuclear or electronic spin operator, is expressed as

$$
A^{\times} = A\otimes 1 - 1\otimes A^{\mathrm{Tr}}, \tag{C1}
$$

where, the superscript Tr implies the transpose of a matrix, $(A^{\mathrm{Tr}})_{ij} = A_{ji}$, 1 is the unity operator, and the symbol $\otimes$ stands for the tensor (or Kroneker, or direct) product between two matrices:

$$
\langle k_1', k_1''|A\otimes B|k_2', k_2''\rangle \equiv \langle k_1'|A|k_2'\rangle\langle k_1''|B|k_2''\rangle. \tag{C2}
$$

In order to consider the Liouville operator for the hyperfine interaction $H_{hf} = \sum_{i=1,2}A_{A_i}$; $A_{A_i} = I_i\cdot A_i\cdot S (i=1,2)$ of the electron spin with the two nuclei, the spherical components of the spin operators $\boldsymbol{I}_i$ and $\boldsymbol{S}$ will be expressed in terms of the spherical tensor of each operator, by transforming the direct product in terms of the resultant spherical tensor in the composite vector space [11]:

$$
\begin{aligned}
A_{A_i}(\ell,m_i) = \sum_{m_{1i},m_{2i}} C(1,1,\ell;m_{1i},m_{2i},m_i)T^{(1,m_1)}_s T^{(1,m_{2i})}_{Ii}, \\
i=1,2;
\end{aligned}
\tag{C3}
$$

where the first-rank spherical components $T^{(1,m)}_{Ii} (i=1,2)$ are defined as follows:

$$
T^{(1,0)}_{Ii} = I_{zi}; \quad T^{(1,\pm1)}_{Ii} = \mp\frac{1}{\sqrt{2}}I_{i\pm} \quad i=1,2 \tag{C4}
$$

and the $C(1,1,\ell;m_{1i},m_{2i},m_i)$ are the Clebsch–Gordan coefficients. The matrix elements of $T^{(\ell,m_i)}_{Ii}$ are expressed as follows:

$$
\begin{aligned}
\langle m^{I_i}_1|T^{(1,m_i)}_{Ii}|m^{I_i}_2\rangle = \delta_{m^{I_i}_1,m_i+m^{I_i}_2}\{m^{I_i}_1\delta_{m_i,0} - m_i\delta_{|m_i|,1}[I_i(I_i+1) \\
- m^{I_i}_1m^{I_i}_2]^{1/2}/\sqrt{2}\} \quad i=1,2.
\end{aligned}
\tag{C5}
$$

The following matrix elements, as derived from the definition of the p and q indices, are required in the calculations that follow:

$$
\begin{aligned}
\langle p^{I_i}_1, q^{I_i}_1|T^{(1,m_i)}_{I_i}\otimes 1|p^{I_i}_2, q^{I_i}_2\rangle &\equiv \left\langle \frac{(q^{I_i}_1+p^{I_i}_1)}{2}\middle| T^{(1,m_i)}_{I_i}\middle|\frac{(q^{I_i}_2+p^{I_i}_2)}{2}\right\rangle \delta_{\frac{(q^{I_i}_1-p^{I_i}_1)}{2},\frac{(q^{I_i}_2-p^{I_i}_2)}{2}} \\
&= \delta_{\Delta p^{I_i},\Delta q^{I_i}}\delta_{\Delta p^{1_i},m_i}\left[\delta_{\Delta p^{I_i},0}\frac{(q^{I_i}_1+p^{I_i}_1)}{2} - \delta_{|\Delta p^{I_i}|,1}\Delta p^{I_i}K_{I_i}/\sqrt{2}\right], \\
i &= 1,2
\end{aligned}
\tag{C6a}
$$

$$\langle p_1^{I_i}, q_1^{I_i}|1\otimes[T_{1_i}^{(1,m_i)}]^{Tr}|p_2^{I_i}, q_2^{I_i}\rangle \equiv \delta_{\frac{q_1^{I_i}+p_1^{I_i}}{2},\frac{q_2^{I_i}+p_2^{I_i}}{2}}\left\langle \frac{(q_1^{I_i}-p_1^{I_i})}{2}\right|T_{I_i}^{(1,m_i)^{Tr}}\left|\frac{(q_2^{I_i}-p_2^{I_i})}{2}\right\rangle$$
$$= \delta_{-\Delta p^{I_i},\Delta q^{I}}\delta_{\Delta p^{I_i},m_i}\left[\delta_{\Delta p^{I_i},0}\frac{(q_1^{I_i}-p_1^{I_i})}{2}-\delta_{|\Delta p^{I_i}|,1}\Delta p^{I_i}K_{I_i}/\sqrt{2}\right],$$
$$i=1,2, \tag{C6b}$$

In the above,

$$\Delta p^{I_i} = p_1^{I_i} - p_2^{I_i},$$
$$\Delta q^{I_i} = q_1^{I_i} - q_2^{I_i},$$
$$K_{Ii} = [I_i(I_i+1) - (q_1^{I_i}\Delta q^{I_i} + p_1^{I_i}\Delta p^{I_i})(q_1^{I_i}\Delta q^{I_i} + p_1^{I_i}\Delta p^{I_i} - 2)/4]^{1/2};$$
$$i = 1,2.$$

One can similarly derive equations analogous to (C4, C5, C6a, C6b) for the electron spin operator.

From Eq. (C3) one can calculate the matrix elements of $[A_{A_i,L}^{(\ell,m)}]^{\times}(i=1,2)$:

$$\langle p_1^s, q_1^s; p_1^{I_1}, q_1^{I_1}; p_1^{I_2}, q_1^{I_2}|[A_{A_i,L}^{(\ell,m)}]^{\times}|p_2^s, q_2^s; p_2^{I_1}, q_2^{I_1}; p_2^{I_2}, q_2^{I_2}\rangle$$
$$= \delta_{m,\Delta p^i}\delta_{|\Delta p^S|,|\Delta q^S|}\delta_{|\Delta p^{I_i}|,|\Delta q^{I_i}|}\delta_{\Delta p^S\Delta p^{I_i},\Delta q^S\Delta q^{I_i}}\delta_{p_1^{I_j},p_2^{I_j}}\delta_{q_1^{I_j},q_2^{I_j}}C(1,1,\ell;\Delta p^S,\Delta p^{I_i},\Delta p^i)S_{Ai};$$
$$= \delta_{m,\Delta p^i}\delta_{|\Delta p^S|,|\Delta q^S|}\delta_{|\Delta p^{I_i}|,|\Delta q^{I_i}|}\delta_{\Delta p^S\Delta p^{I_i},\Delta q^S\Delta q^{I_i}}\delta_{p_1^{I_j},p_2^{I_j}}\delta_{q_1^{I_j},q_2^{I_j}}(-1)^{\Delta p^i}(2\ell+1)^{1/2}\begin{pmatrix}1 & 1 & \ell\\ |\Delta p^S| & \Delta p^{I_i} & -\Delta p^i\end{pmatrix}S_{Ai};$$
$$(i,j) = (1,2),(2,1), \tag{C7}$$

Eq. (C7) includes the expressions obtained by using the 3-j symbol for the Clebsch–Gordan coefficient [17]. In Eq. (C7), $j=2$, 1 for $i=1$, 2, respectively; $\Delta p^s = p_1^s - p_2^s$; $\Delta q^s = q_1^s - q_2^s$; $\Delta p^i \equiv \Delta p^S + \Delta p^{I_i}$; $i=1,2$; and the quantity S_{Ai} (i= 1,2) assumes the following possible values:

$$\Delta p^S = 0, \Delta p^{I_i} = 0 : S_{Ai} = (p_1^S q_1^{I_i} + p_1^{I_i} q_1^S)/2;$$
$$\Delta p^S = 0, \Delta p^{I_i} \neq 0 : S_{Ai} = -(p_1^S\Delta p^{I_i} + q_1^S\Delta q^{I_i})K_{Ii}/\sqrt{8};$$
$$\Delta p^S \neq 0, \Delta p^{I_i} = 0 : S_{Ai} = -(p_1^{I_i}\Delta p^S + q_1^{I_i}\Delta q^S)/\sqrt{8};$$
$$\Delta p^S \neq 0, \Delta p^{I_i} \neq 0 : S_{Ai} = \Delta p^S\Delta q^{I_i}K_{Ii}/2. \tag{C7a}$$

Similarly, one can derive the matrix elements of $[A_{g,L}^{(\ell,m)}]^{\times}$ [11,17]:

$$\langle p_1^s, q_1^s; p_1^{I_1}, q_1^{I_1}; p_1^{I_2}, q_1^{I_2}|[A_{g,L}^{(\ell,m)}]^{\times}|p_2^s, q_2^s; p_2^{I_1}, q_2^{I_1}; p_2^{I_2}, q_2^{I_2}\rangle$$
$$= \delta_{\Delta p^{I_1},0}\delta_{\Delta q^{I_1},0}\delta_{\Delta p^{I_2},0}\delta_{\Delta q^{I_2},0}\delta_{|\Delta p|,|\Delta q|}\delta_{\Delta p^S,m}B_0C(1,1,\ell;\Delta p,0,\Delta p)S_g$$
$$= \delta_{\Delta p^{I_1},0}\delta_{\Delta q^{I_1},0}\delta_{\Delta p^{I_2},0}\delta_{\Delta q^{I_2},0}\delta_{|\Delta p|,|\Delta q|}\delta_{\Delta p^S,m}B_0(-1)^{\Delta p}(2\ell+1)^{1/2}$$
$$\times\begin{pmatrix}1 & 1 & \ell\\ \Delta p & 0 & -\Delta p\end{pmatrix}\left\{p_1^s\delta_{\Delta p^S,0} - \Delta q^S(1-\delta_{\Delta p^S,0})/\sqrt{2}\right\}, \tag{C8}$$

where

$$\Delta p = \Delta p^S + \Delta p^{I_1} + \Delta p^{I_2};$$
$$\Delta q = \Delta q^S + \Delta q^{I_1} + \Delta q^{I_2}$$

and S_g is defined as

$$\Delta p^S = 0: \ S_g = p_1^S;$$
$$\Delta p^S \neq 0: \ S_g = -\Delta q^S/\sqrt{2}. \tag{C8a}$$

The matrix elements given by Eqs. (C7) and (C8) have the following symmetry properties:

$$\langle -p_1^s, q_1^s; -p_1^{I_1}, q_1^{I_1}; -p_1^{I_2}, q_1^{I_2}|[A_{\mu,L}^{(\ell,-m)}]^{\times}$$
$$|-p_2^s, q_2^s; -p_2^{I_1}, q_2^{I_1}; -p_2^{I_2}, q_2^{I_2}\rangle$$
$$= (-1)^{1+\Delta p}\langle p_1^s, q_1^s; p_1^{I_1}, q_1^{I_1}; p_1^{I_2}, q_1^{I_2}|[A_{\mu,L}^{(\ell,m)}]^{\times}|p_2^s, q_2^s; p_2^{I_1}, q_2^{I_1}; p_2^{I_2}, q_2^{I_2}\rangle. \tag{C9}$$

In the same fashion, the matrix elements of the two nuclear Zeeman interactions, $[A_{n_i,L}^{(0,0)}]^{\times}$; $i=1,2$, are expressed as [17]:

$$\langle p_1^s, q_1^s; p_1^{I_1}, q_1^{I_1}; p_1^{I_2}, q_1^{I_2}|[A_{n_i,L}^{(\ell,m_i)}]^{\times}|p_2^s, q_2^s; p_2^{I_1}, q_2^{I_1}; p_2^{I_2}, q_2^{I_2}\rangle$$
$$= \delta_{m_i,0}\delta_{\Delta p^S,0}\delta_{\Delta q^S,0}\delta_{\Delta p^{I_1},0}\delta_{\Delta q^{I_1},0}\delta_{\Delta p^{I_2},0}\delta_{\Delta q^{I_2},0}Bp_1^{I_i}. \tag{C10}$$

References

[1] J.H. Freed, Theory of slow tumbling ESR spectra for nitroxides, in: L. Berliner (Ed.), Spin Labeling: Theory and Applications, vol. 1, Academic Press, New York, 1976, pp. 53–132, Chapter 3.

[2] G. Moro, J.H. Freed, Calculation of ESR spectra and related Fokker–Planck forms by the use of the Lanczo's algorithm, J. Chem. Phys. 74 (1981) 3757–3773.

[3] K.V. Vasavada, D.J. Schneider, J.H. Freed, J. Chem. Phys. 86 (1987) 647.

[4] Z. Liang, Y. Lou, J.H. Freed, L. Clumbus, W.L. Hubbell, J. Phys. Chem. 108 (2004) 17649–17659.

[5] A. Polimino, J.H. Freed, J. Phys. Chem. 99 (1995) 10995–11006.

[6] Z. Liang, Y. Lou, J.H. Freed, J. Phys. Chem. B 103 (1999) 6384.

[7] J.P. Barnes, Z. Liang, H.S. Mchaourab, J.H. Freed, W.L. Hubbel, Biophys. J. 76 (1999) 3298.

[8] J.H. Freed, ESR and molecular dynamics, in: S.S. Eaton, G.R. Eaton, L.J. Berliner (Eds.), Biological Magnetic Resonance, vol. 24, Kluwer, New York, 2005, 239–268.

[9] P.P. Borbat, A.J. Costa-Filho, K.A. Earle, J.A. Mocicki, J.H. Freed, Science 291 (2001) 266.

[10] V. Barone, A. Polimeno, Phys. Chem. Chem. Phys. 8 (2006) 4609, and references cited therein.

[11] E. Meirovitch, D. Igner, E. Igner, G. Moro, J.H. Freed, J. Chem. Phys. 77 (1982) 3915–3938.

[12] G. Moro, EPRLF and EPRLP routines, unpublished report, Cornell University, Ithaca, New York, 1980.

[13] G. Moro, Implementation of the Lanczo's algorithm in the calculation of spectral functions, unpublished report, Cornell University, Ithaca, New York, 1980.

[14] G. Moro, J.H. Freed, J. Chem. Phys. 74 (1981) 3757.

[15] D.J. Schneider, J.H. Freed, Calculating slow motional magnetic resonance spectra: a user's guide, in: L. Berliner, J. Reuben (Eds.), Biological Magnetic Resonance, vol. 6, Plenum Publishing Corporation, 1989, pp. 1–75.
[16] D.J. Schneider, J.H. Freed, Adv. Chem. Phys. 73 (1989) 387.
[17] S. Lee, D. Budil, J.H. Freed, J. Chem. Phys. 101 (1994) 5529–5558.
[18] K.A. Earle, D.E. Budil, in: Shulamit Schlick (Ed.), Advanced ESR Methods in Polymer Research, John Wiley and Sons, New York, 2006.
[19] L. Cataldo, C. Dutan, S.K. Misra, S. Loss, H. Grutzmacher, M. Geoffroy, Chem. Eur. J. 11 (2005) 3463–3468.
[20] J.H. Freed, private communication, 2007.